

Patuxent Tributary Summary:
**A summary of trends in tidal water quality and
associated factors, 1985-2018.**

June 7, 2021

Prepared for the Chesapeake Bay Program (CBP) Partnership by the CBP
Integrated Trends Analysis Team (ITAT)



This tributary summary is a living document in draft form and has not gone through a formal peer review process. We are grateful for contributions to the development of these materials from the following individuals: Jeni Keisman, Rebecca Murphy, Olivia Devereux, Jimmy Webber, Qian Zhang, Meghan Petenbrink, Tom Butler, Zhaoying Wei, Jon Harcum, Renee Karrh, Mike Lane, and Elgin Perry.

Contents

1. Purpose and Scope.....	3
2. Location.....	4
2.1 Watershed Physiography	4
2.2 Land Use.....	6
2.3 Tidal Waters and Stations	8
3. Tidal Water Quality Dissolved Oxygen Criteria Attainment.....	9
4. Tidal Water Quality Trends	12
4.1 Surface Total Nitrogen	13
4.2 Surface Total Phosphorus	16
4.3 Surface Chlorophyll <i>a</i> : Spring (March-May).....	18
4.4 Surface Chlorophyll <i>a</i> : Summer (July-Sept)	20
4.5 Secchi Disk Depth.....	22
4.6 Summer Bottom Dissolved Oxygen (June-September).....	24
5. Factors Affecting Trends	25
5.1 Watershed Factors.....	25
5.1.1 Effects of Physical Setting	25
5.1.2 Estimated Nutrient and Sediment Loads	28
5.1.3 Expected Effects of Changing Watershed Conditions.....	30
5.1.4 Best Management Practices (BMPs) Implementation.....	33
5.1.5 Flow-Normalized Watershed Nutrient and Sediment Loads	34
5.2 Tidal Factors	34
5.3 Insights on Changes in the Patuxent.....	38
6. Summary	38
References	39
Appendix	43

1. Purpose and Scope

The Patuxent Tributary Summary outlines change over time in a suite of monitored tidal water quality parameters and associated potential drivers of those trends for the time period 1985 – 2018, and provides a brief description of the current state of knowledge explaining these observed changes. Water quality parameters described include surface (above pycnocline) total nitrogen (TN), surface total phosphorus (TP), spring and summer (June, July, August) surface chlorophyll *a*, summer bottom (below pycnocline) dissolved oxygen (DO) concentrations, and Secchi disk depth (a measure of water clarity). Results for annual surface water temperature, bottom TP, bottom TN, surface ortho-phosphate (PO₄), surface dissolved inorganic nitrogen (DIN), surface total suspended solids (TSS), and summer surface DO concentrations are provided in an Appendix. Drivers discussed include physiographic watershed characteristics, changes in nitrogen, phosphorus, and sediment loads from the watershed to tidal waters, expected effects of changing land use, and implementation of nutrient management and natural resource conservation practices. Factors internal to estuarine waters that also play a role as drivers are described including biogeochemical processes, physical forces such as wind-driven mixing of the water column, and biological factors such as phytoplankton biomass and the presence of submersed aquatic vegetation. Continuing to track water quality response and investigating these influencing factors are important steps to understanding water quality patterns and changes in the Patuxent River.

2. Location

The Patuxent River watershed covers approximately 1.4% of the Chesapeake Bay watershed. Its watershed is approximately 2,236 km² (Table 1.) and is contained within one state, Maryland (Figure 1).

Tributary Name	Watershed Area km2
MARYLAND MAINSTEM	71967
POTOMAC	36611
JAMES	25831
YORK	6537
RAPPAHANNOCK	6530
LOWER EASTERN SHORE	4532
MARYLAND UPPER EASTERN SHORE	2441
PATUXENT	2236
VIRGINIA MAINSTEM	2052
CHOPTANK	1844
PATAPSCO-BACK	1647
MARYLAND UPPER WESTERN SHORE	1523
MARYLAND LOWER WESTERN SHORE	439

Table 1. "Watershed areas for each of the thirteen tributary or tributary groups for which Tributary Trends summaries have been produced. All of the tributary summaries can be accessed at the following link: <https://cast.chesapeakebay.net/Home/TMDLTracking#tributaryRptsSection>".

2.1 Watershed Physiography

The Patuxent River watershed stretches across two major physiographic regions, namely, Piedmont and Coastal Plain (Bachman *et al.*, 1998) (Figure 1). The Piedmont physiography covers primarily crystalline areas. The Coastal Plain physiography covers lowland, dissected upland, and upland areas. Implications of these physiographies for nutrient and sediment transport are summarized in Section 5.1.1.

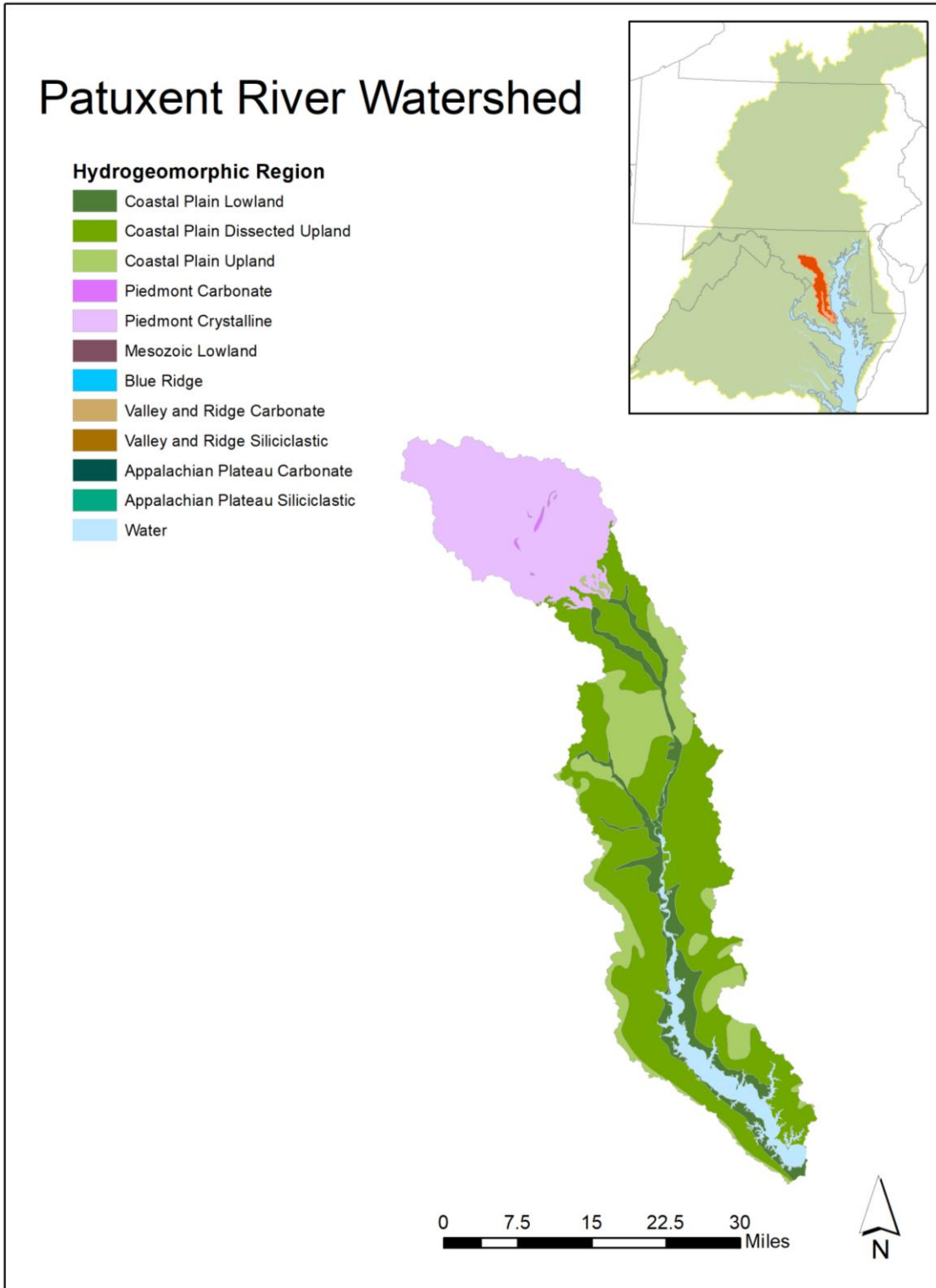


Figure 1. Distribution of physiography in the Patuxent River watershed. Base map credit Chesapeake Bay Program, www.chesapeakebay.net, North American Datum 1983.

2.2 Land Use

Land use in the Patuxent watershed is dominated (54%) by natural areas. Urban and suburban land areas have increased by 86,149 acres since 1985, agricultural lands have decreased by 44,543 acres, and natural lands have decreased by 41,713 acres. Correspondingly, the proportion of urban land in this watershed has increased from 17% in 1985 to 33% in 2019 (Figure 2).

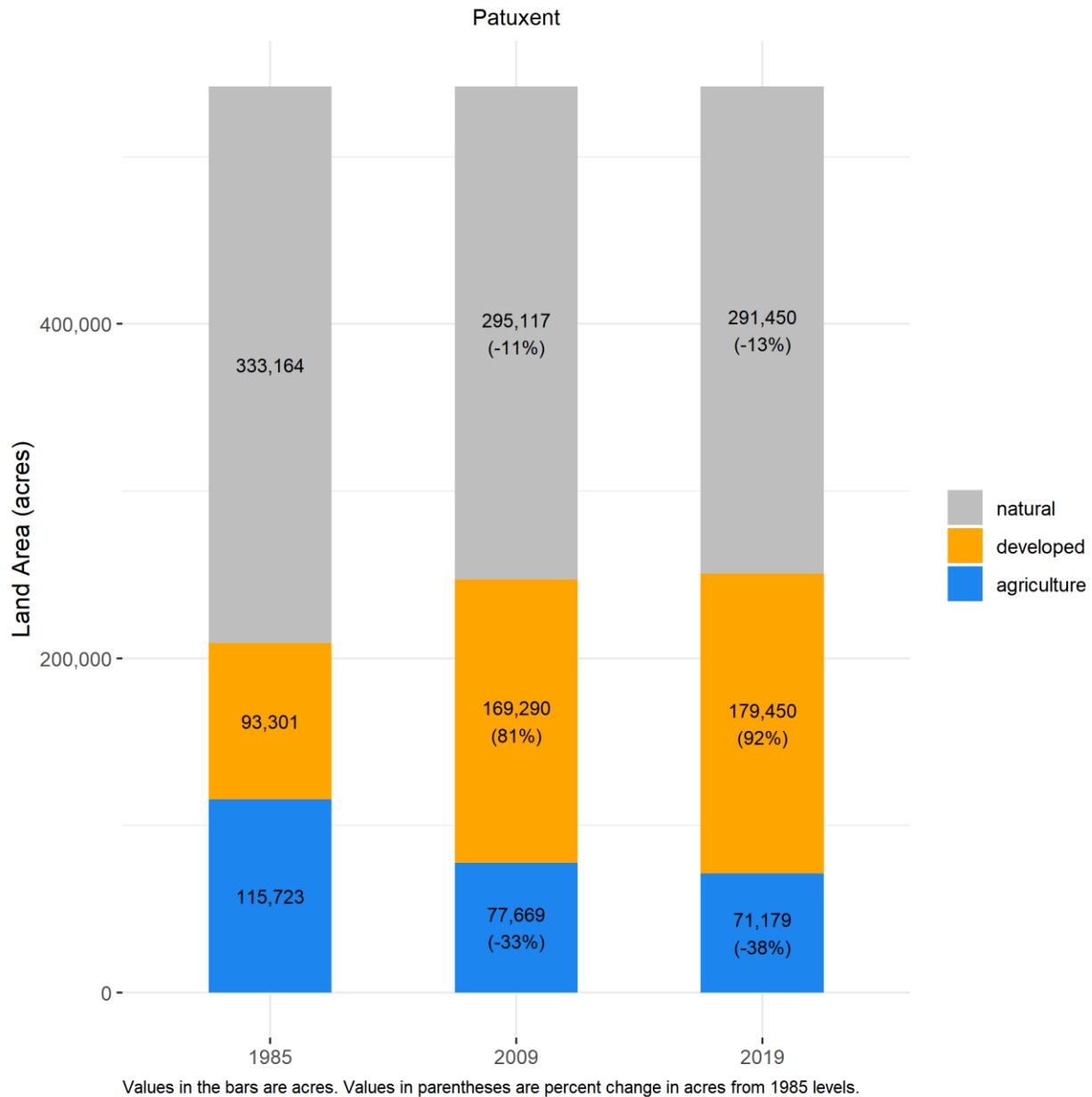


Figure 2. Distribution of land uses in the Patuxent watershed. Percentages are the percent change from 1985 for each source sector.

In general, developed lands in the 1970s were concentrated within towns and major metropolitan areas. Since then, developed and semi-developed lands have increased around these areas, as well as

expanding into previously undeveloped regions (Figure 3). The impacts of land development differ depending on the use from which the land is converted (Keisman *et al.*, 2019; Ator *et al.*, 2019). Implications of changing land use for nutrient and sediment transport are summarized in Section 5.1.3.

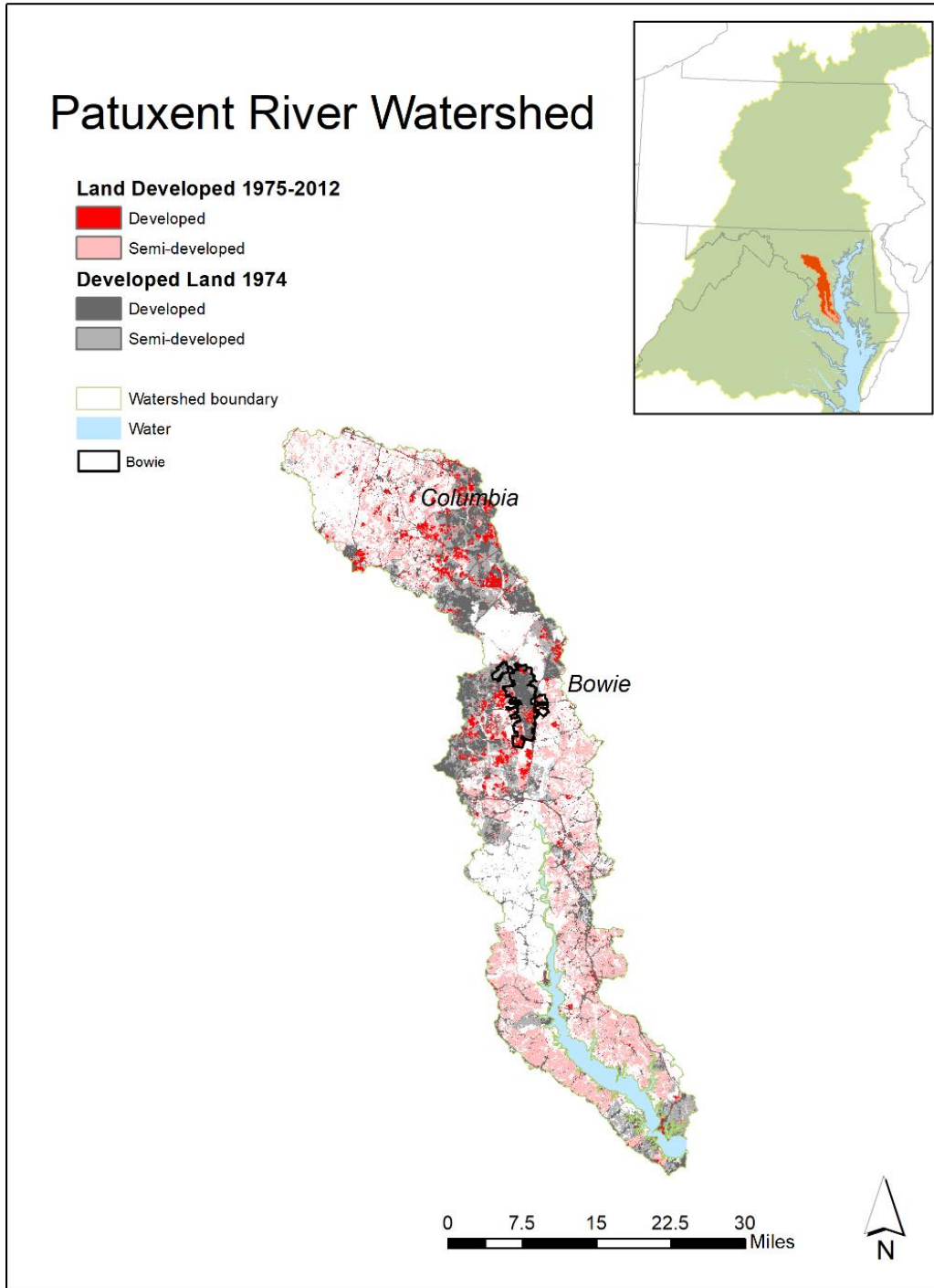


Figure 3. Distribution of developed land in the Patuxent River watershed. Derived from Falcone (2015). Base map credit Chesapeake Bay Program, www.chesapeakebay.net, North American Datum 1983.

2.3 Tidal Waters and Stations

For the purposes of water quality standards assessment and reporting, the tidal waters associated with the Patuxent River and the Western Branch tributary are divided into four segments (U.S. Environmental Protection Agency, 2004): Tidal Fresh Western Branch and Patuxent (WBRTF, PAXTF), Oligohaline Patuxent River (PAXOH), and the Mesohaline Patuxent River (PAXMH) (Figure 4).

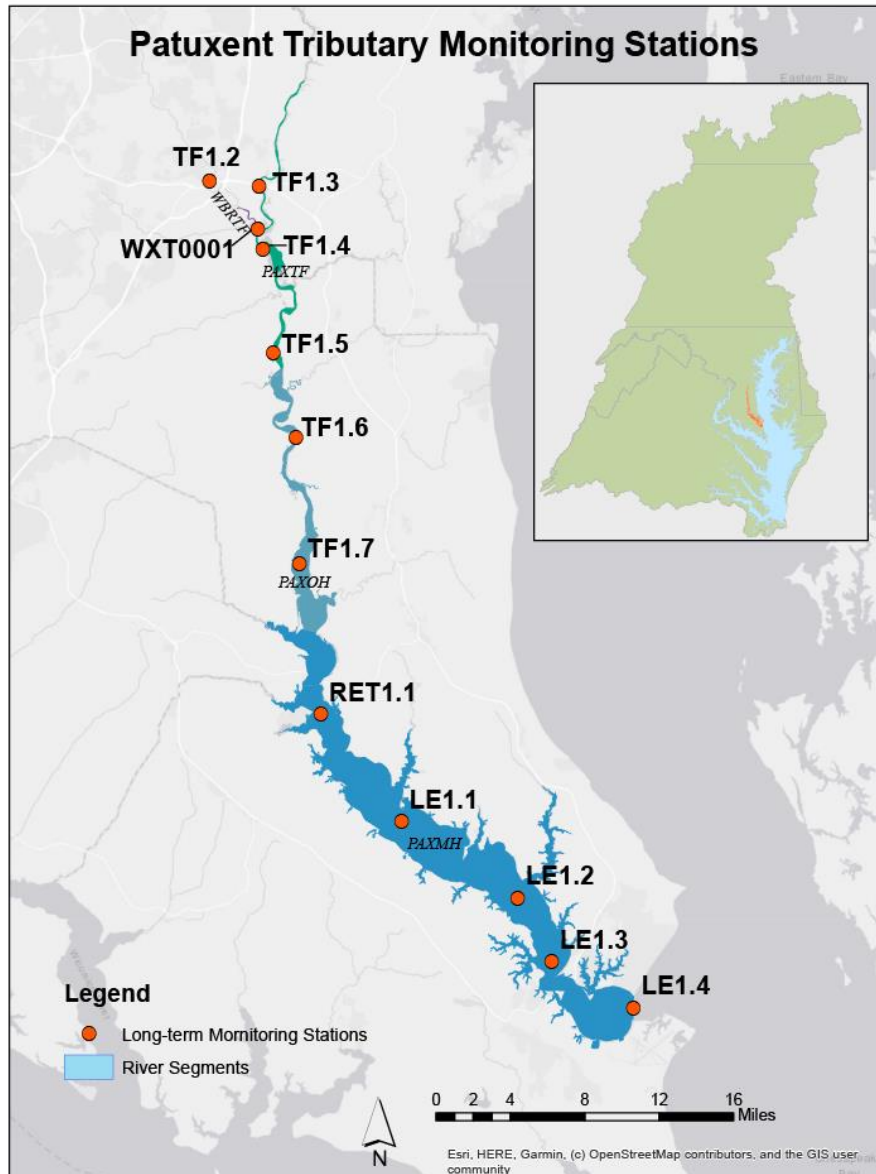


Figure 4. Map of tidal Patuxent River segments and long-term monitoring stations. Base map credit Esri, HERE, Garmin, (c) OpenStreetMap contributors, and the GIS user community, World Geodetic System 1984.

Long-term trends in water quality are analyzed by MD Department of Natural Resources at 12 stations stretching from the Western Branch to of the mouth of the Patuxent flowing into Chesapeake Bay (Figure 4). Water quality data at these stations are also used to assess attainment of dissolved oxygen (DO) water quality criteria. All tidal water quality data analyzed for this summary are available from the Chesapeake Bay Program Data Hub (Chesapeake Bay Program, 2018). Other shallow-water monitoring has been conducted over the years and used for water quality criteria evaluation but is not shown in the long-term trend graphics in subsequent sections because of its shorter duration.

3. Tidal Water Quality Dissolved Oxygen Criteria Attainment

Multiple water quality standards were developed for the Patuxent River and Western Branch to protect aquatic living resources (U.S. Environmental Protection Agency, 2003; Tango and Batiuk, 2013). These standards include specific criteria for dissolved oxygen (DO) and water clarity/underwater bay grasses. For the purposes of this summary, a record of the evaluation results indicating whether each of the tributary segments have met or not met either 30-day or instantaneous Open Water (OW) and Deep Water (DW) DO criteria over time is shown below (Zhang *et al.*, 2018a; Hernandez Cordero *et al.*, 2020). While analysis of water quality standards attainment is not the focus of this summary, the results (Tables 2 and 3) provide context for the importance of understanding factors affecting water quality trends. For more information on water quality standards, criteria, and standards attainment, visit the CBP’s “Chesapeake Progress” website at www.chesapeakeprogress.com. In the recent period (2016-2018), none of the segments met the 30-day mean OW summer DO requirement, nor did the mesohaline Patuxent segment (PAXMH) met the 30-day mean DW summer DO requirement (Zhang *et al.*, 2018b).

Table 2. Open Water summer DO criterion evaluation results (30-day mean June-September assessment period). Green indicates that the criterion was met. White indicates that the criterion was not met. “ND” indicates no data.

time period	WBRTF	PAXTF	PAXOH	PAXMH
1985-1987	ND			
1986-1988	ND			
1987-1989	ND			
1988-1990	ND			
1989-1991				
1990-1992				
1991-1993				
1992-1994				
1993-1995				
1994-1996				
1995-1997				
1996-1998				
1997-1999				
1998-2000				

1999-2001				
2000-2002				
2001-2003				
2002-2004				
2003-2005				
2004-2006				
2005-2007				
2006-2008				
2007-2009				
2008-2010				
2009-2011				
2010-2012				
2011-2013				
2012-2014				
2013-2015				
2014-2016				
2015-2017				
2016-2018				

Table 3. Deep Water summer DO (30-day mean) criteria evaluation results. Green indicates that the criterion was met. White indicates that the criterion was not met. (Note: the entire table is white intentionally because this criterion has not been met during this period.)

time period	PAXMH
1985-1987	
1986-1988	
1987-1989	
1988-1990	
1989-1991	
1990-1992	
1991-1993	
1992-1994	
1993-1995	
1994-1996	
1995-1997	
1996-1998	
1997-1999	
1998-2000	
1999-2001	
2000-2002	
2001-2003	
2002-2004	
2003-2005	
2004-2006	
2005-2007	
2006-2008	
2007-2009	
2008-2010	
2009-2011	
2010-2012	

2011-2013	
2012-2014	
2013-2015	
2014-2016	
2015-2017	
2016-2018	

Comparing trends in station-level DO concentrations to the computed DO criterion status for a recent assessment period can reveal valuable information, such as whether progress is being made towards attainment in a segment that is not meeting the water quality criteria, or conversely the possibility that conditions are degrading even if the criteria are currently being met. To illustrate this, the 2016-2018 attainment status for the OW summer and DW summer DO criteria shown in Tables 2 and 3 are overlain with the 1985-2018 change in summer surface DO concentration and the 1985-2018 change in bottom summer DO concentrations, respectively (Figure 5). The bottom depths at each of these stations is different due to varying bathymetry, but the bottom DO trends at these stations are expected to represent water in the DW designated use. As mentioned above, none of the applicable criteria were met in the 2016-2018 period. Degrading surface oxygen concentrations in the WBRTF and PAXTF segments indicate lack of progress towards meeting those criteria. Improving surface DO in the PAXMH region, does indicate positive progress there; however, two stations with bottom DO decreases show that this improvement is not consistent throughout the water column.

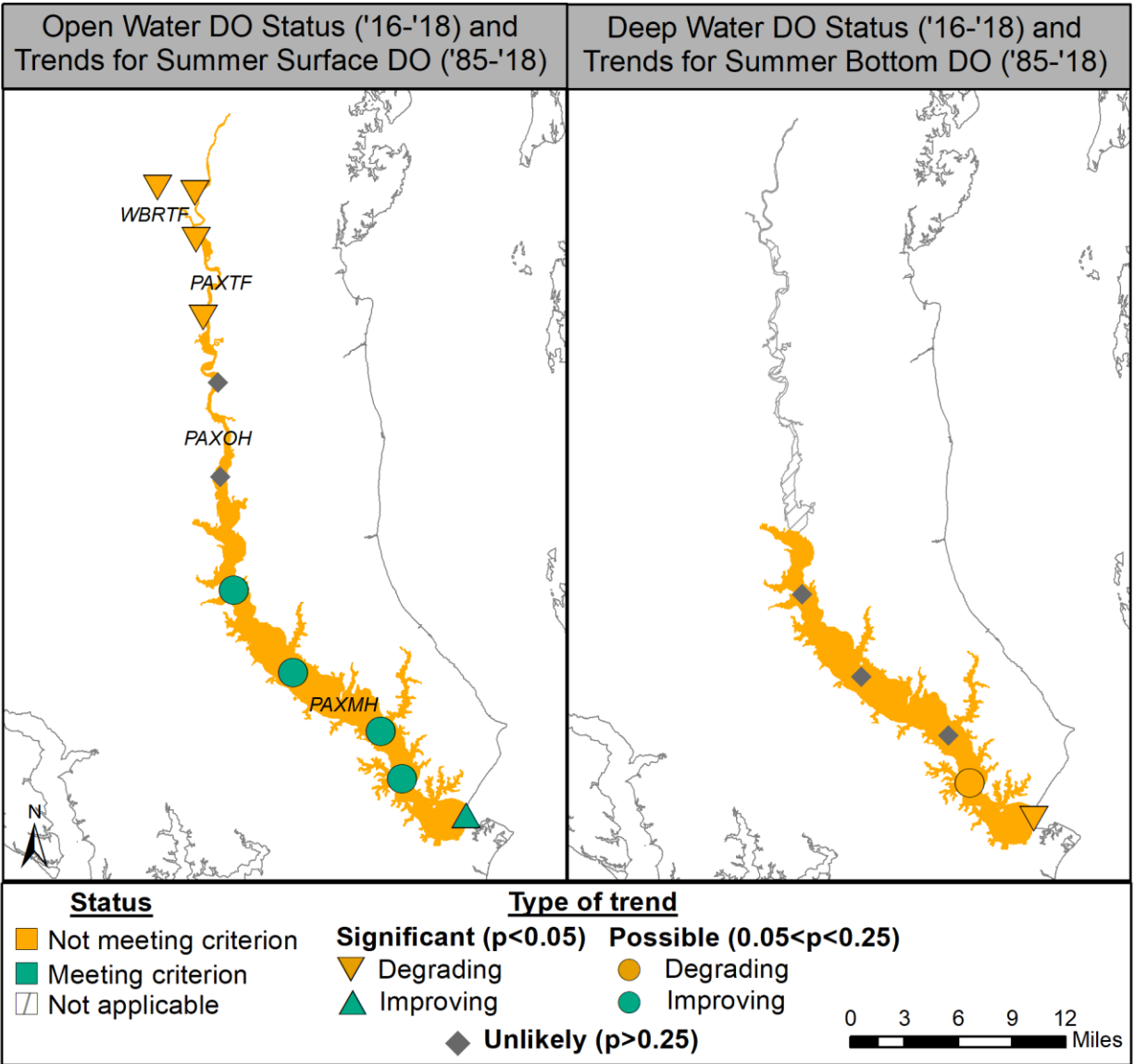


Figure 5. Pass-fail DO criterion status for 30-day OW summer DO and DW summer DO designated uses in Patuxent segments along with long-term trends in DO concentrations. Base map credit Chesapeake Bay Program, www.chesapeakebay.net, North American Datum 1983.

4. Tidal Water Quality Trends

Tidal water quality trends are computed by fitting generalized additive models (GAMs) to the water quality observations that have been collected one or two times per month since the 1980s at the 12 Patuxent River and Western Branch stations labeled in Figure 4. For more details on the GAM implementation that is applied each year by MD Department of Natural Resources for these stations in collaboration with the Chesapeake Bay Program and Virginia analysts, see Murphy *et al.* (2019).

Results shown below in each set of maps (e.g., Figure 6) include those generated using two different GAM fits to each station-parameter combination. The first approach involves fitting a GAM to the raw

observations to generate a mean estimate of the concentrations over time, as observed in the estuary. The second approach involves including monitored river flow or *in situ* salinity (as an aggregated measure of multiple river flows) in the GAM to explain some of the variation in the water quality parameter. From the results of this second approach, it is possible to estimate the “flow-adjusted” change over time, which gives a mean estimate of what the water quality parameter trend would have been if river flow had been average over the period of record. Note that depending on station and parameter, sometimes gaged river flow is used for this adjustment and sometimes salinity is used, but we refer to all these results as “flow-adjusted” for simplicity.

To determine if there has been a change over time (i.e., a trend) at a particular station for a given parameter, we compute a percent change between the estimates at beginning and end of a period of interest from the GAM fit. For each percent change computation, the level of statistical confidence can be computed as well. Change is called significant if $p < 0.05$ and possible if the p-value is up to 0.25. That upper limit is higher than usually reported for hypothesis tests but allows us to provide a more complete picture of the results, identifying locations where change might be starting to occur and should be investigated (Murphy *et al.*, 2019). In addition to the maps of trends, for each parameter, there is a set of graphs (e.g., Figure 7) that include the raw observations (dots on the graphs) and lines representing the mean annual or seasonal GAM estimates, without flow-adjustment. The flow-adjusted GAM line graphs are not shown.

4.1 Surface Total Nitrogen

Annual total nitrogen (TN) trends have decreased over the long-term at every Patuxent River station, with and without flow-adjustment (Figure 6). Over the short-term, the improvements are limited mostly to the upper half of the river, with more improvements after flow-adjustment than without flow-adjustment.

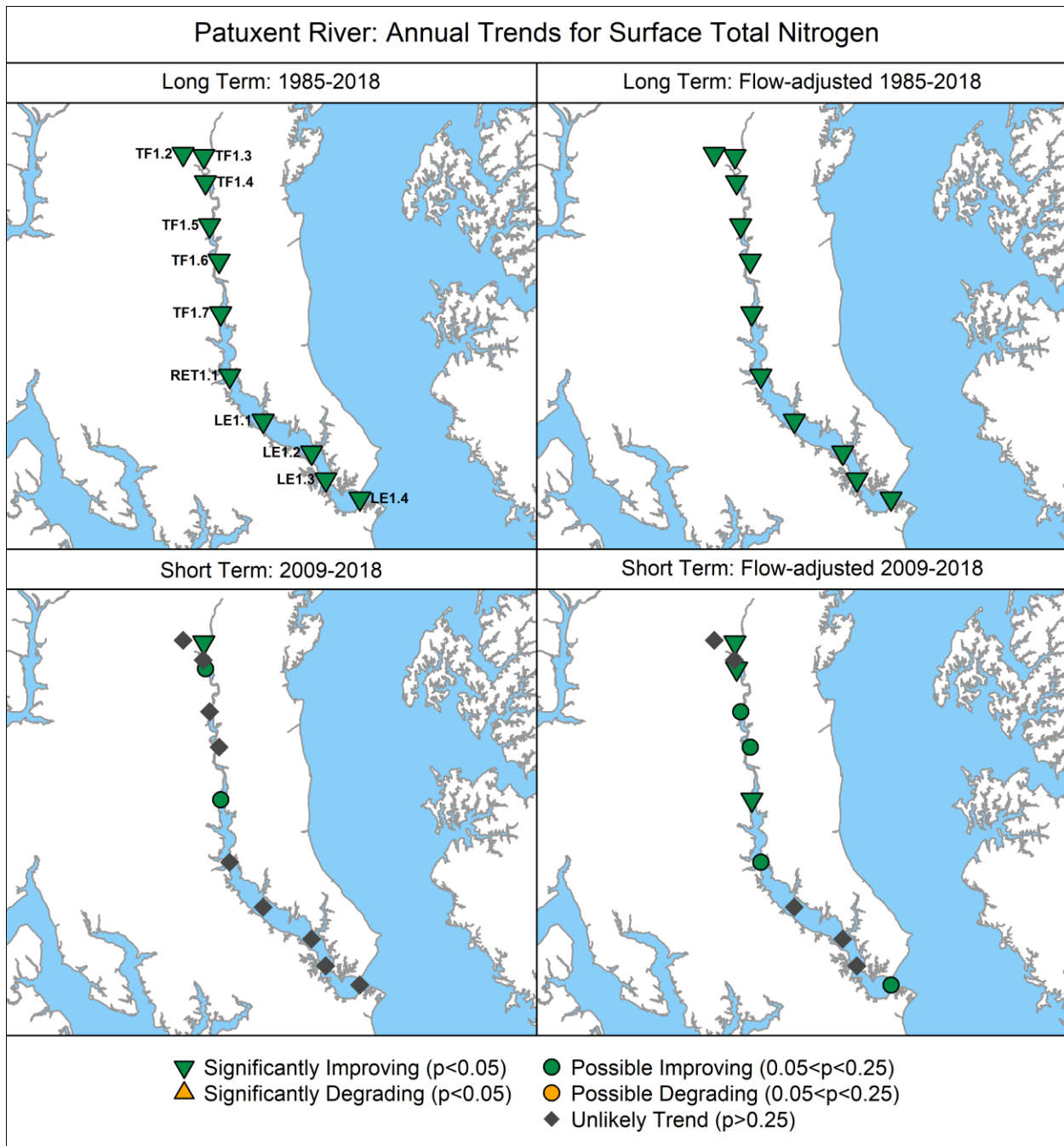


Figure 6. Surface TN trends. Base map credit Chesapeake Bay Program, www.chesapeakebay.net, North American Datum 1983.

TN data values and mean annual GAM estimates decreased dramatically in the 1980s and early 1990s for the tidal fresh and oligohaline stations in the Patuxent River and Western Branch (Figure 7). The long-term decreases are less obvious at the mesohaline stations where the magnitude of the TN concentrations are also lower than they are in the tidal fresh. Vertical blue dotted lines represent a laboratory and method change (July 1, 1990) that was tested for its impact on data values. A statistical

intervention test within the GAM models showed that these changes were significant at the stations in the bottom panel (Figure 7). This is evident by the vertical jump in the mean annual GAM estimates shown with the lines. With this technique, we can estimate long-term change after accounting for the artificial jump from the method change (Murphy *et al.*, 2019).

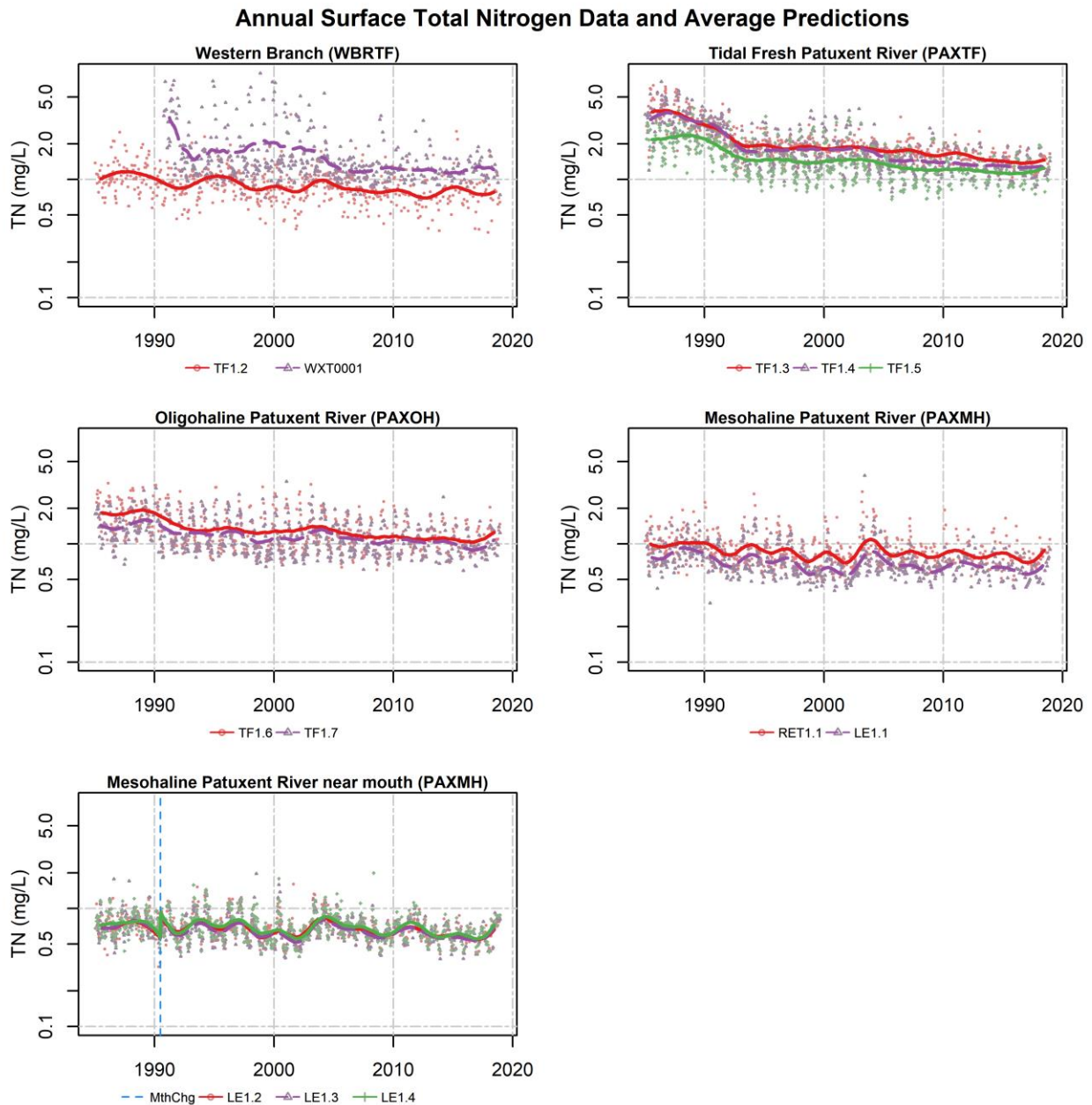


Figure 7. Surface TN data (dots) and average long-term pattern generated from non-flow adjusted GAM. Colored dots represent data corresponding to the monitoring station shown indicated in the legend; colored lines represent mean annual GAM estimates for the noted monitoring stations. Vertical blue dotted lines represent timing of changes in laboratory and/or sampling methods.

4.2 Surface Total Phosphorus

Surface total phosphorus (TP) trends are improving at every Patuxent River and Western Branch station over the long-term, both with and without flow-adjustment (Figure 8). Over the short-term, the picture changes and all of the stations except for the freshest four stations and LE1.4 have degrading trends, with and without flow-adjustment (Figure 8).

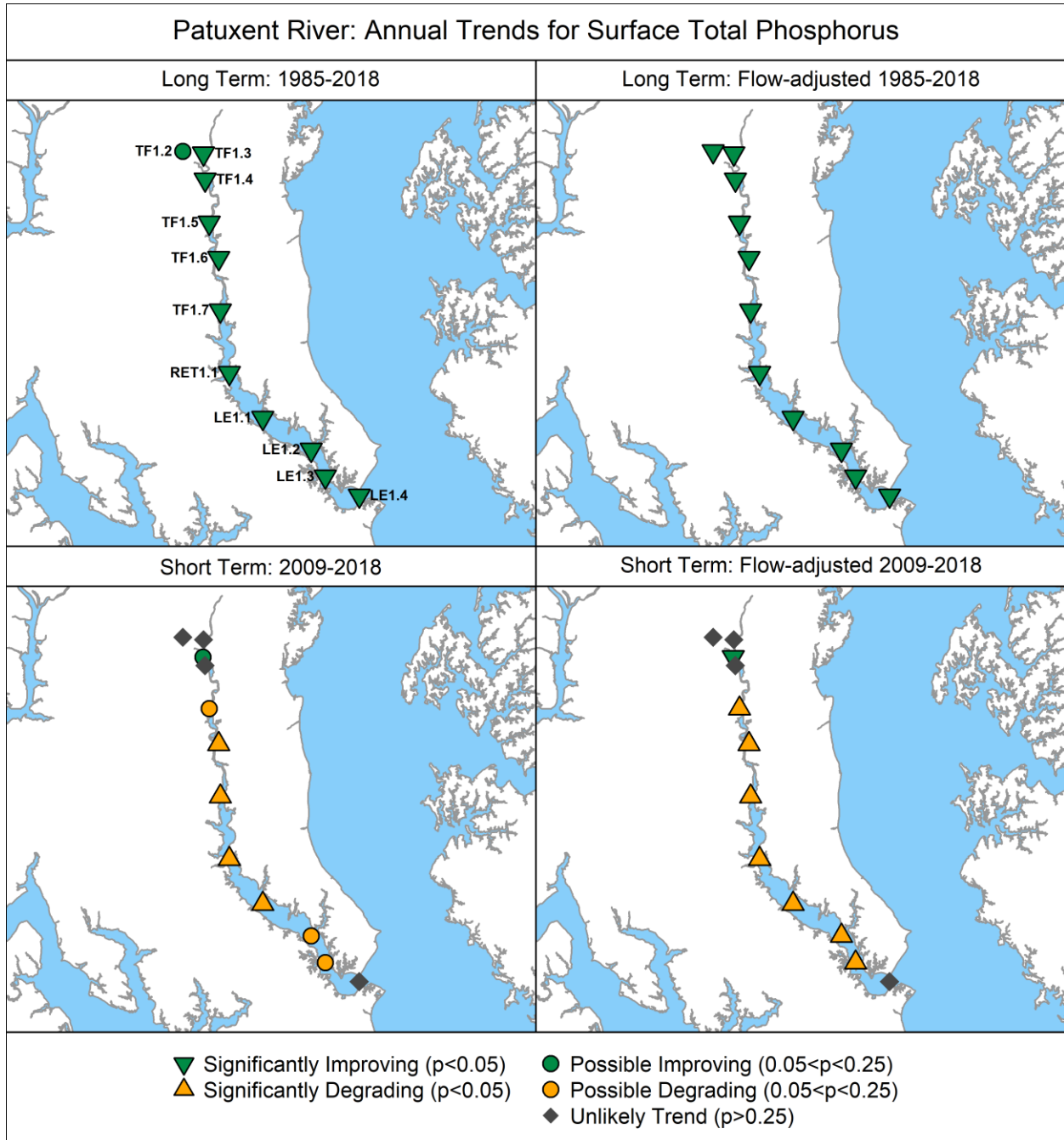


Figure 8. Surface TP trends. Base map credit Chesapeake Bay Program, www.chesapeakebay.net, North American Datum 1983.

Long-term decreases in TP concentrations and mean annual GAM estimates appear to be mostly driven by large decreases in the first part of the record for these stations (Figure 9). The pattern appears to level out after the initial decrease, especially at the oligohaline and mesohaline stations. The upswing in TP in the last few years at these stations results in the short-term degrading trends shown in Figure 8.

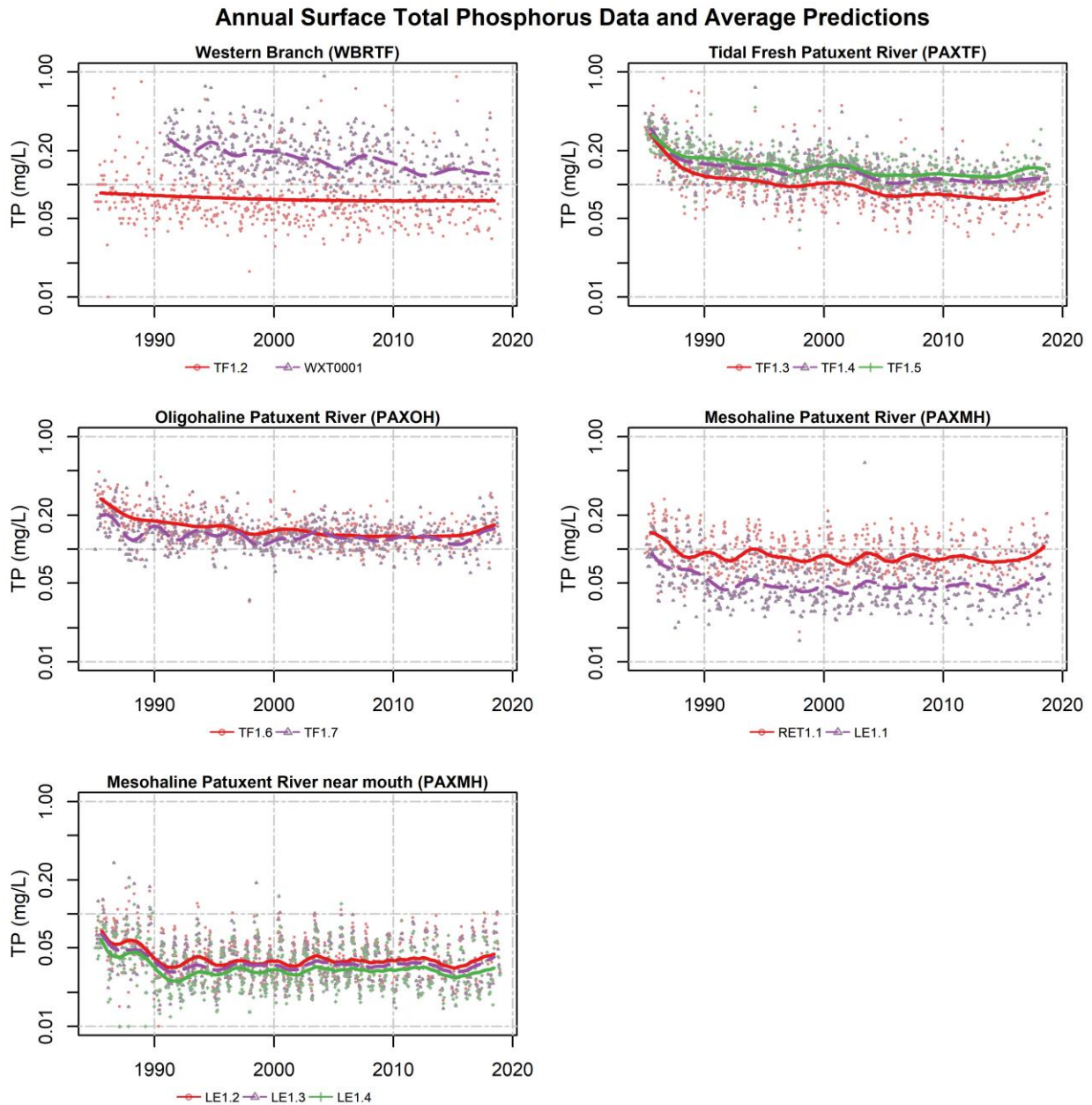


Figure 9. Surface TP data (dots) and average long-term pattern generated from non-flow adjusted GAMs. Colored dots represent data corresponding to the monitoring station shown indicated in the legend; colored lines represent mean annual GAM estimates for the noted monitoring stations.

4.3 Surface Chlorophyll *a*: Spring (March-May)

Trends for chlorophyll *a* are split into spring and summer to analyze chlorophyll *a* during the two seasons when phytoplankton blooms are commonly observed in different parts of Chesapeake Bay (Smith and Kemp, 1995; Harding and Perry, 1997). Spring chlorophyll *a* trends are degrading over the long-term at all of the mesohaline stations (RET1.1 to LE1.4) without flow adjustment, as well as TF1.4 (Figure 10). With flow-adjustment over the long-term, the pattern shifts slightly with more of the tidal fresh stations showing possible degrading trends and LE1.1, LE1.2, and LE1.3 with no trend. Over the short-term, both with and without flow-adjustment, degradations are occurring at several tidal fresh stations (Figure 10).

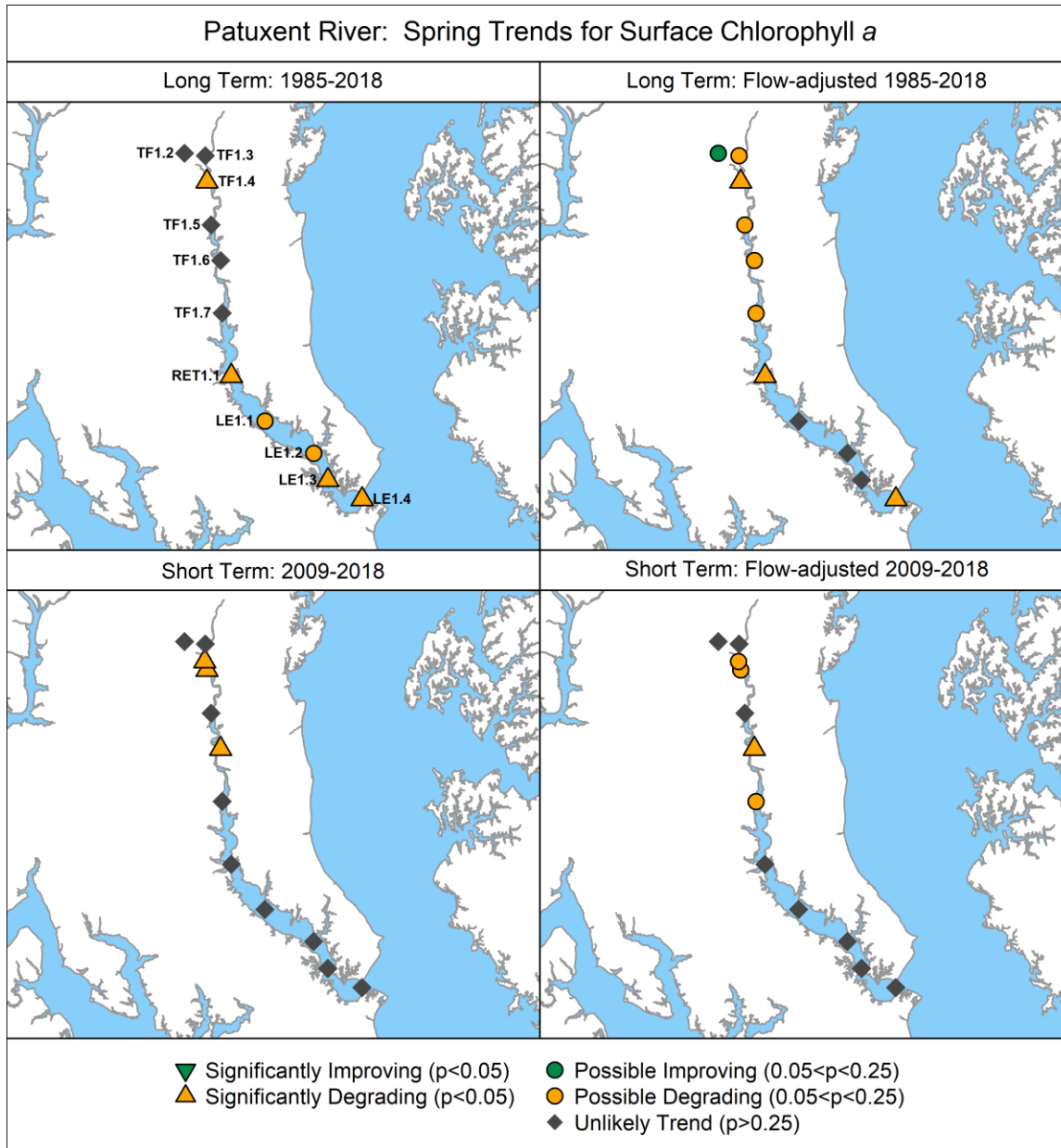


Figure 10. Surface spring (March-May) chlorophyll *a* trends. Base map credit Chesapeake Bay Program, www.chesapeakebay.net, North American Datum 1983.

Spring chlorophyll *a* increases are apparent at most of the stations, with the tidal fresh and oligohaline Patuxent stations also having a slight drop down in the early 2000s (Figure 11). The Western Branch stations (TF1.2 and WXT0001) do not appear to be trending like the main Patuxent stations.

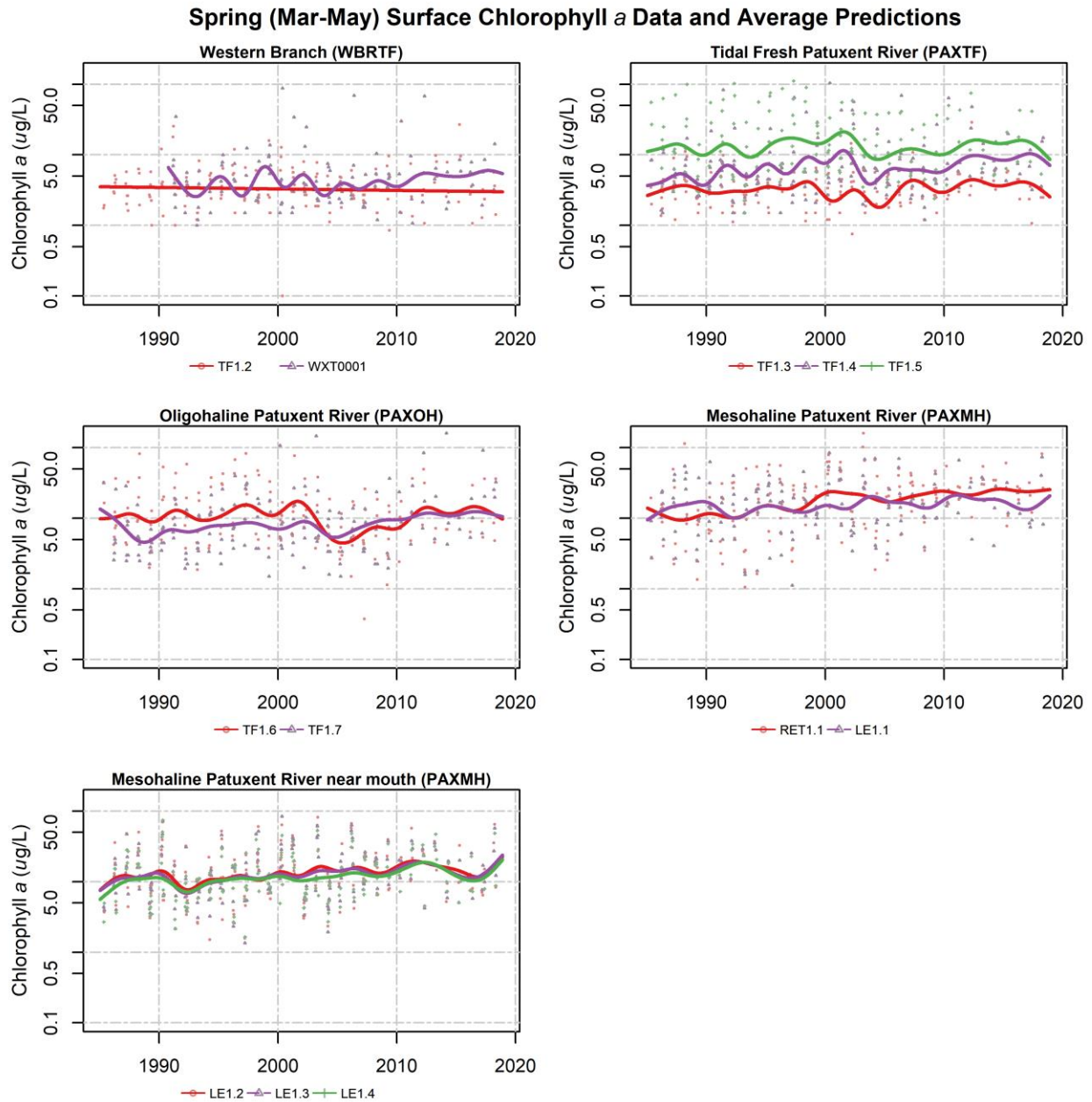


Figure 11. Surface spring chlorophyll *a* data (dots) and average long-term pattern generated from non-flow adjusted GAMs. Colored dots represent March-May data corresponding to the monitoring station indicated in the legend; colored lines represent mean spring GAM estimates for the noted monitoring stations.

4.4 Surface Chlorophyll *a*: Summer (July-Sept)

Summer long-term chlorophyll *a* trends are improving over the long-term at several of the tidal fresh stations without flow-adjustment – including the Western Branch (TF1.2) (Figure 12). With flow-adjustment, TF1.2 is still improving, but the other stations become either no trend or degrading. Over the short-term, both with and without flow-adjustment, the improving trend at TF1.2 continues. The other tidal fresh stations change from mostly no trend in the short-term without adjustment to degrading with flow-adjustment. The mesohaline stations (RET1.1 to LE1.4) are mostly degrading over the long-term, with no trend over the short-term (Figure 12).

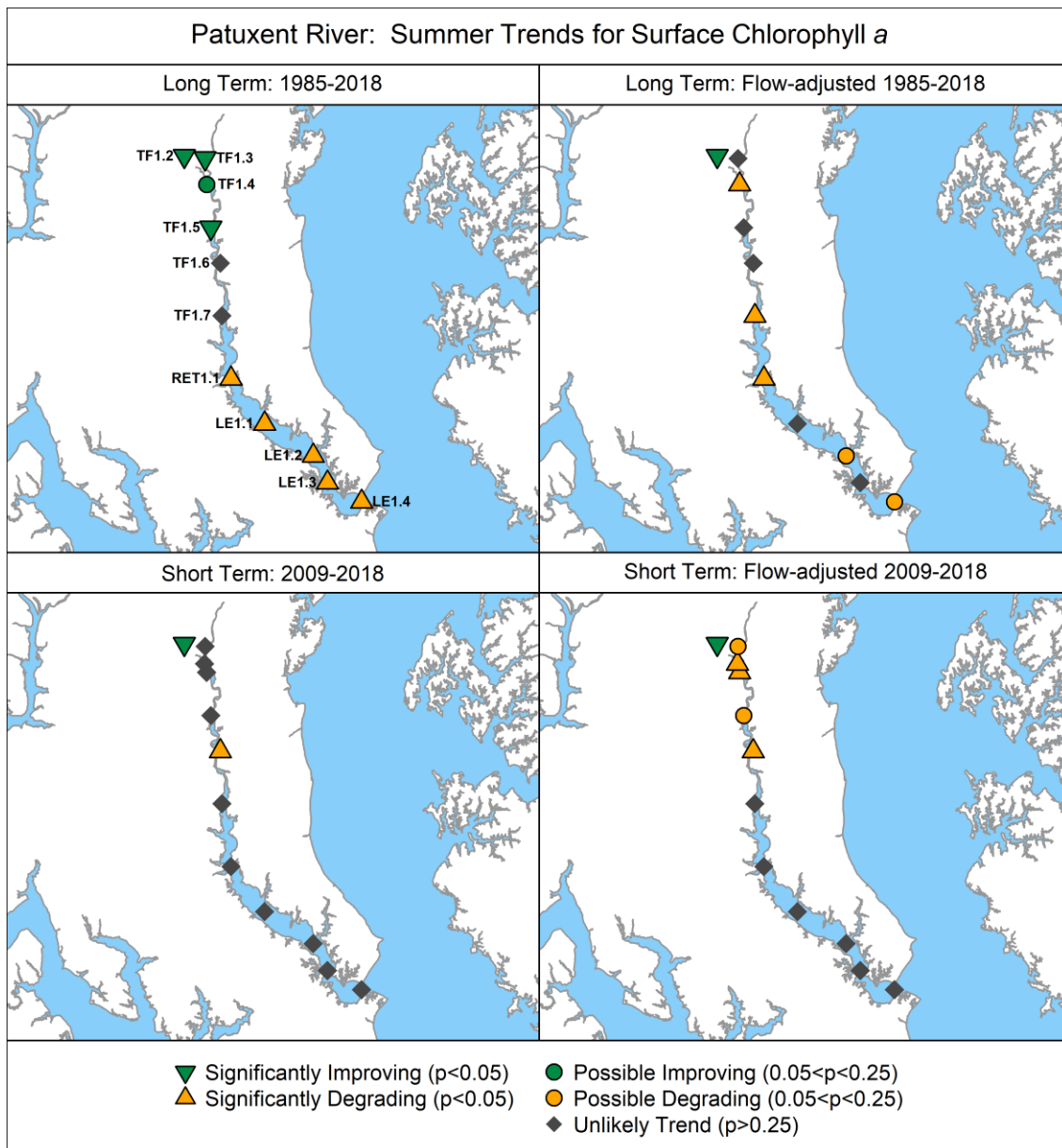


Figure 12. Surface summer (July-September) chlorophyll *a* trends. Base map credit Chesapeake Bay Program, www.chesapeakebay.net, North American Datum 1983.

The magnitude of the summer chlorophyll *a* concentrations at the tidal fresh and oligohaline stations (Figure 13) is higher than the magnitude of the spring concentrations (Figure 11). Also decreases over time are apparent in the summer long-term patterns at TF1.2, WXT0001, TF1.4 and TF1.5 (Figure 13). These summer tidal fresh patterns are subtly different from the spring patterns at the same stations which do not have the clear step-down or decreasing slope over time (Figure 11). The mesohaline stations' long-term patterns, however, are increasing in the summer (Figure 13), consist with the spring.

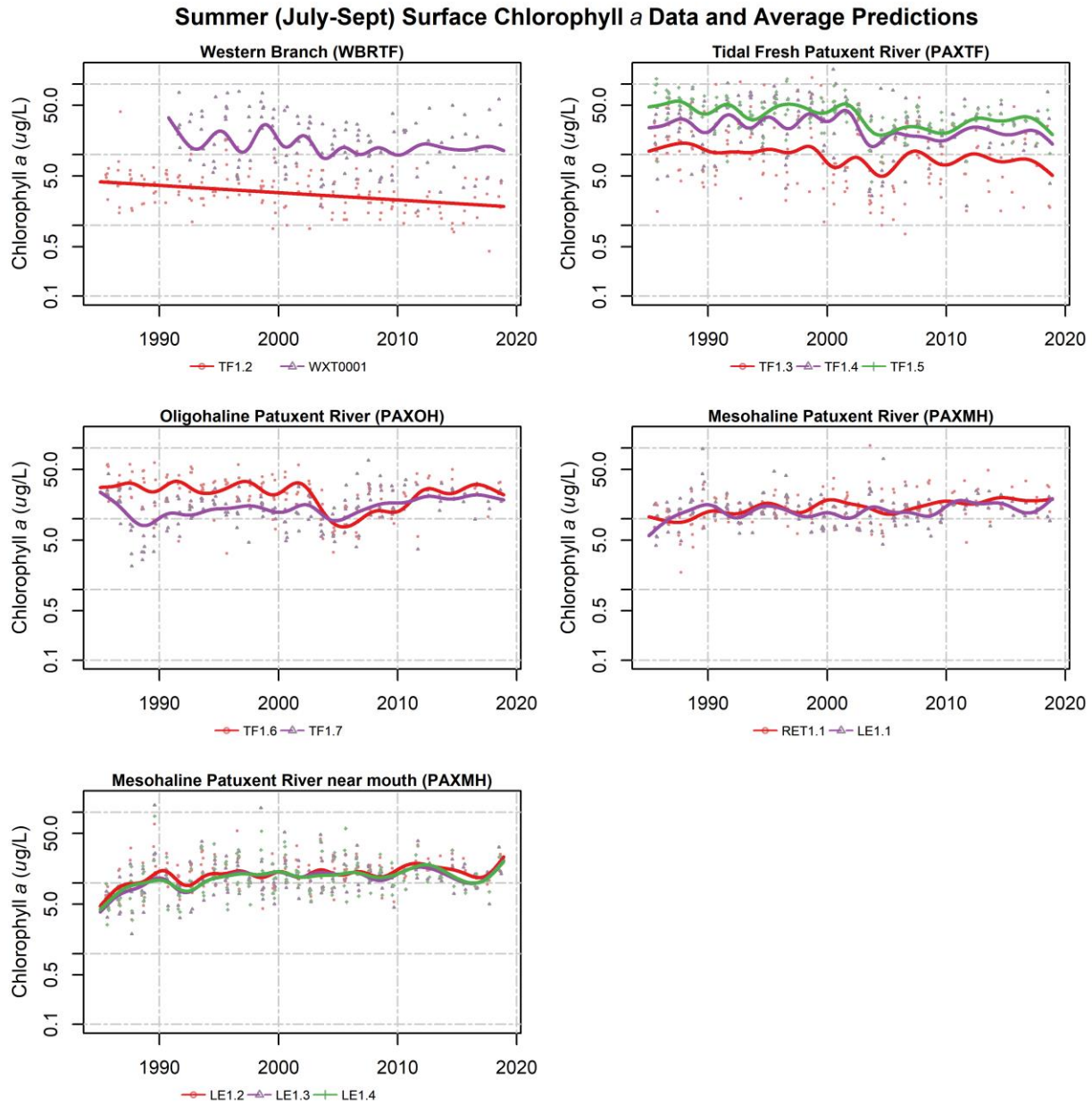


Figure 13. Surface summer chlorophyll *a* data (dots) and average long-term pattern generated from non-flow adjusted GAMs. Colored dots represent July-September data corresponding to the monitoring station indicated in the legend; colored lines represent mean summer GAM estimates for the noted monitoring stations.

4.5 Secchi Disk Depth

Trends in Secchi disk depth, a measure of visibility through the water column, are degrading at most of the stations over the long-term, although some of that degradation in the mesohaline region appears to be explained by flow-adjustment (Figure 14). Over the short-term, there are degrading trends at the tidal fresh and oligohaline stations both with and without flow-adjustment. The mesohaline stations mostly have no trend over the short-term without flow adjustment, and improving trends with flow-adjustment (Figure 14).

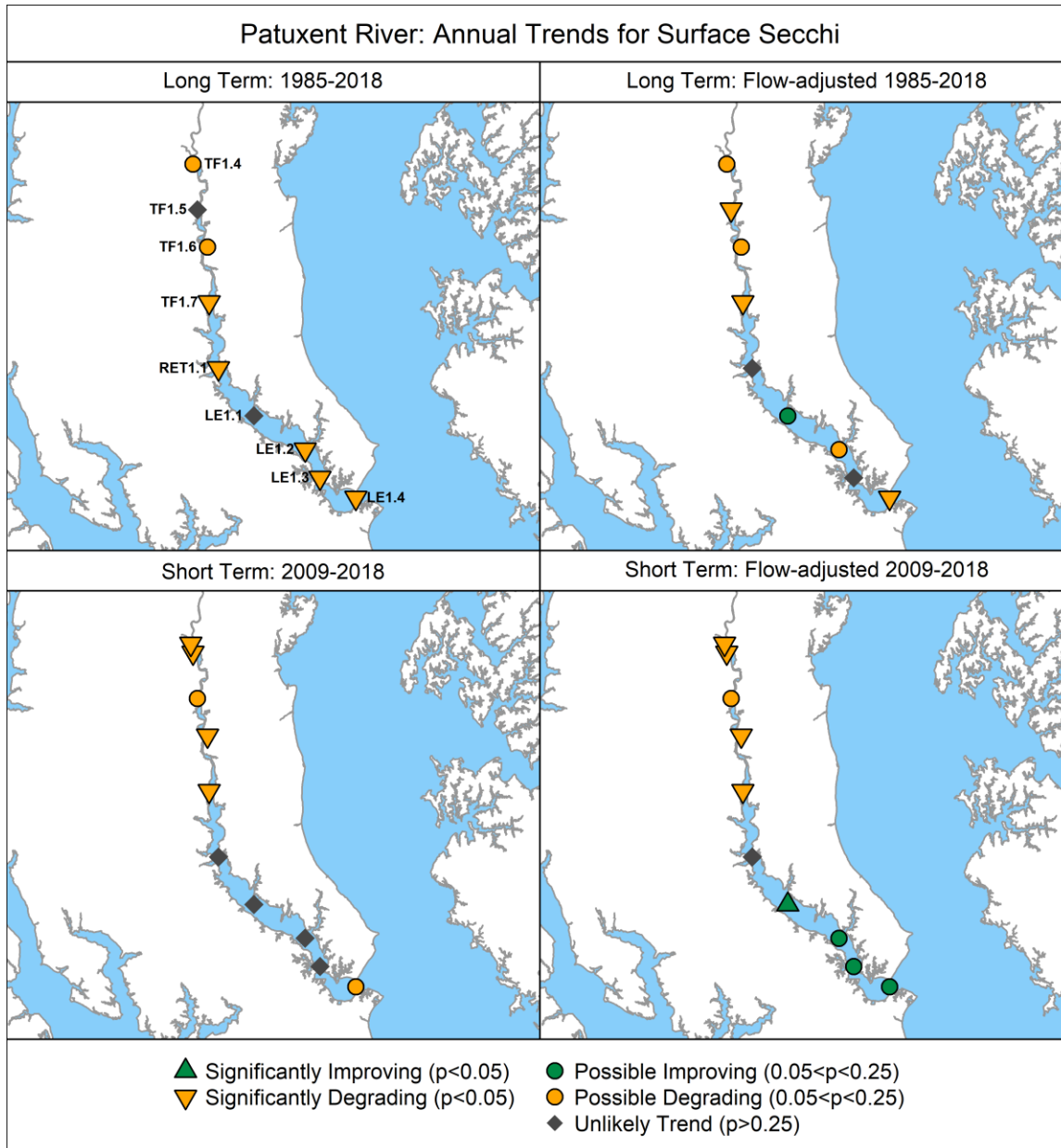


Figure 14. Annual Secchi depth trends. Base map credit Chesapeake Bay Program, www.chesapeakebay.net, North American Datum 1983.

Secchi depth is generally less than 1-meter throughout the tidal fresh and oligohaline stations, and then increases slightly in the mesohaline regions of the Patuxent River (Figure 15). It is difficult to distinguish the changes over time represented by the trends (Figure 14), although a long-term decrease in Secchi depths in the lower mesohaline stations (bottom panel) is apparent, with a leveling-out at the end (Figure 15).

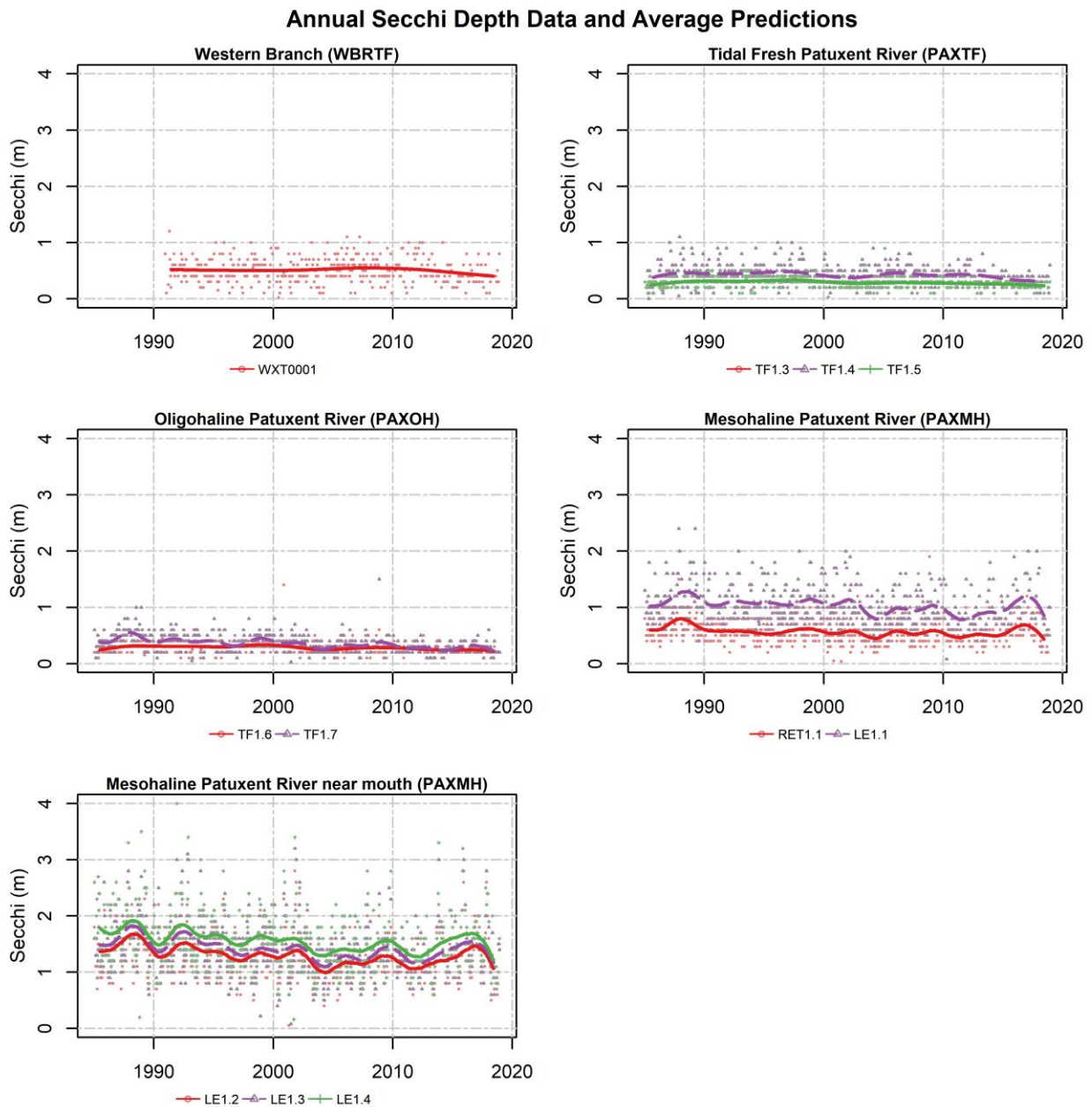


Figure 15. Annual Secchi depth data (dots) and average long-term pattern generated from non-flow adjusted GAMs. Colored dots represent data corresponding to the monitoring station shown indicated in the legend; colored lines represent mean annual GAM estimates for the noted monitoring stations.

4.6 Summer Bottom Dissolved Oxygen (June-September)

Patuxent summer bottom DO has no trend over the long-term at most of the stations, with the exception of long-term degradations at TF1.5 without flow-adjustment and LE1.3 and LE1.4 both with the without flow-adjustment (Figure 16). Over the short-term, more stations show improving trends. With flow-adjustment 6 of the 8 stations have short-term improvements.

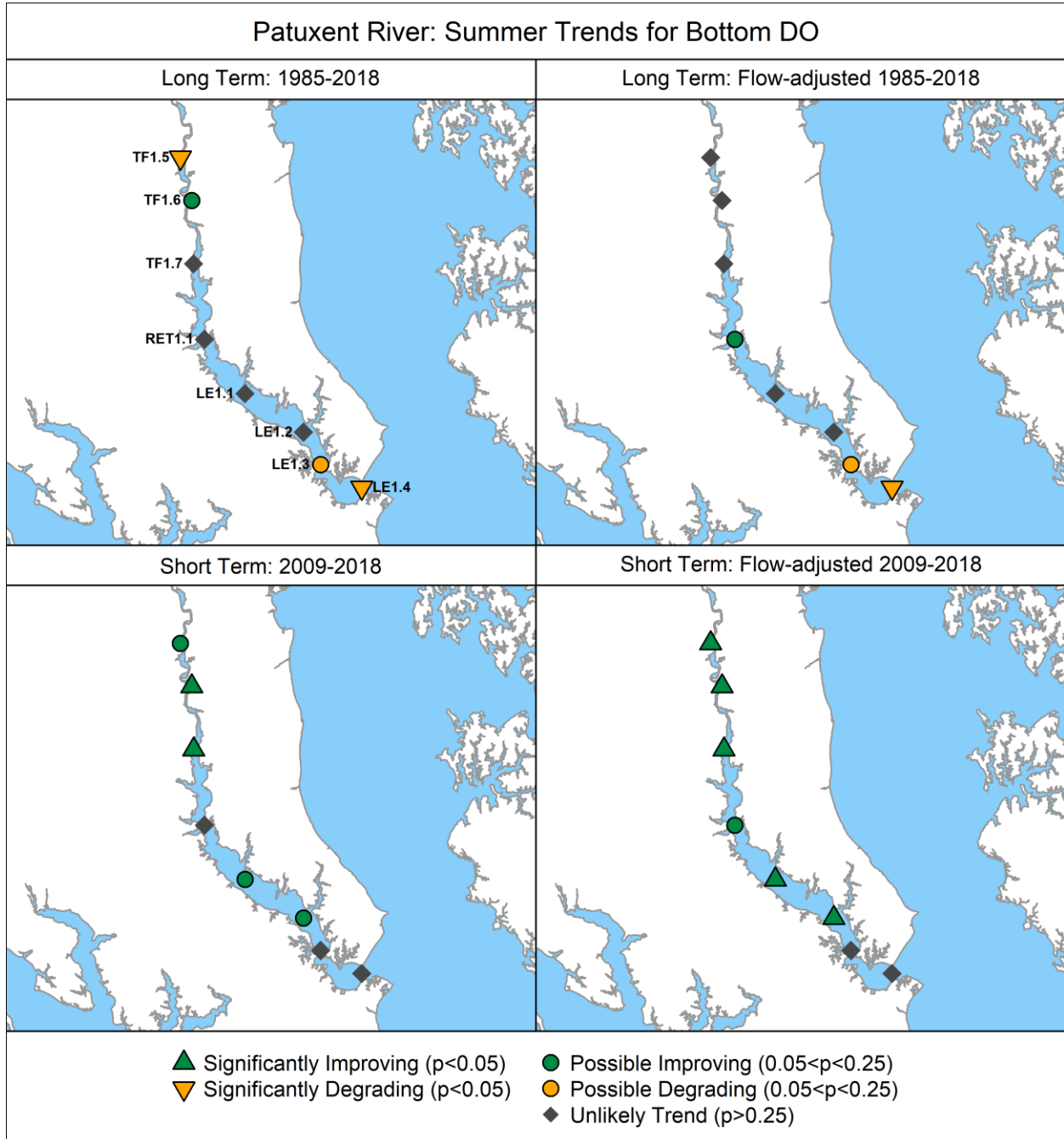


Figure 16. Summer (June-September) bottom DO trends. Base map credit Chesapeake Bay Program, www.chesapeakebay.net, North American Datum 1983.

A long-term decrease is clear in the summer bottom DO data and seasonal mean GAM estimates at TF1.5 (Figure 17). The long-term decrease in concentrations is actually a feature of the patterns at all of the stations. Over the last decade, however, almost all of the GAM estimates have turned upward (Figure 17), leading to the improving short-term trends (Figure 16).

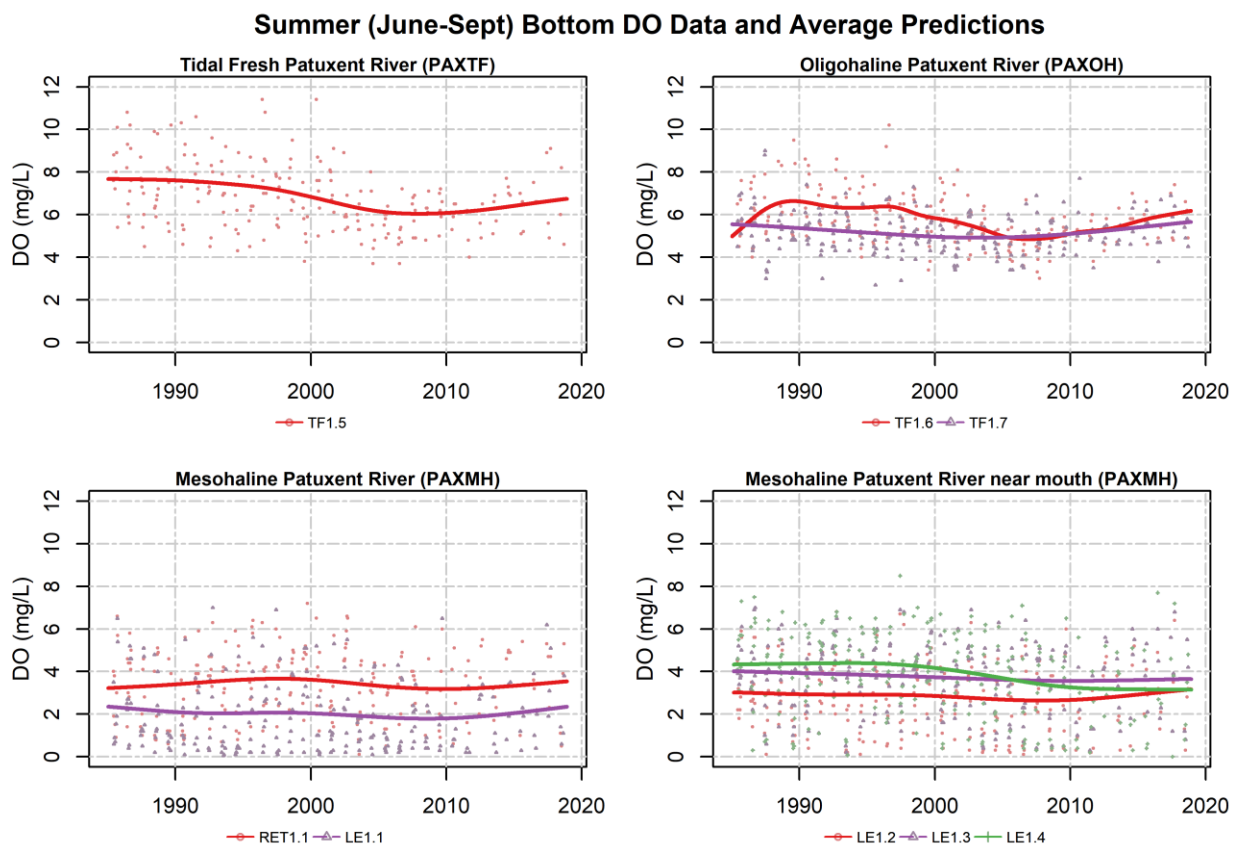


Figure 17. Summer (June-September) bottom DO data (dots) and mean seasonal long-term pattern generated from non-flow adjusted GAMs. Colored dots represent June-September data corresponding to the monitoring station indicated in the legend; colored lines represent mean summer GAM estimates for the noted monitoring stations.

5. Factors Affecting Trends

5.1 Watershed Factors

5.1.1 Effects of Physical Setting

The geology of the Patuxent River watershed and its associated land use affects the quantity and transmissivity of nitrogen, phosphorus, and sediment delivered to non-tidal and tidal streams (Figure 18) (Brakebill *et al.*, 2010; Ator *et al.*, 2011; Ator *et al.*, 2019; Ator *et al.*, 2020; Noe *et al.*, 2020).

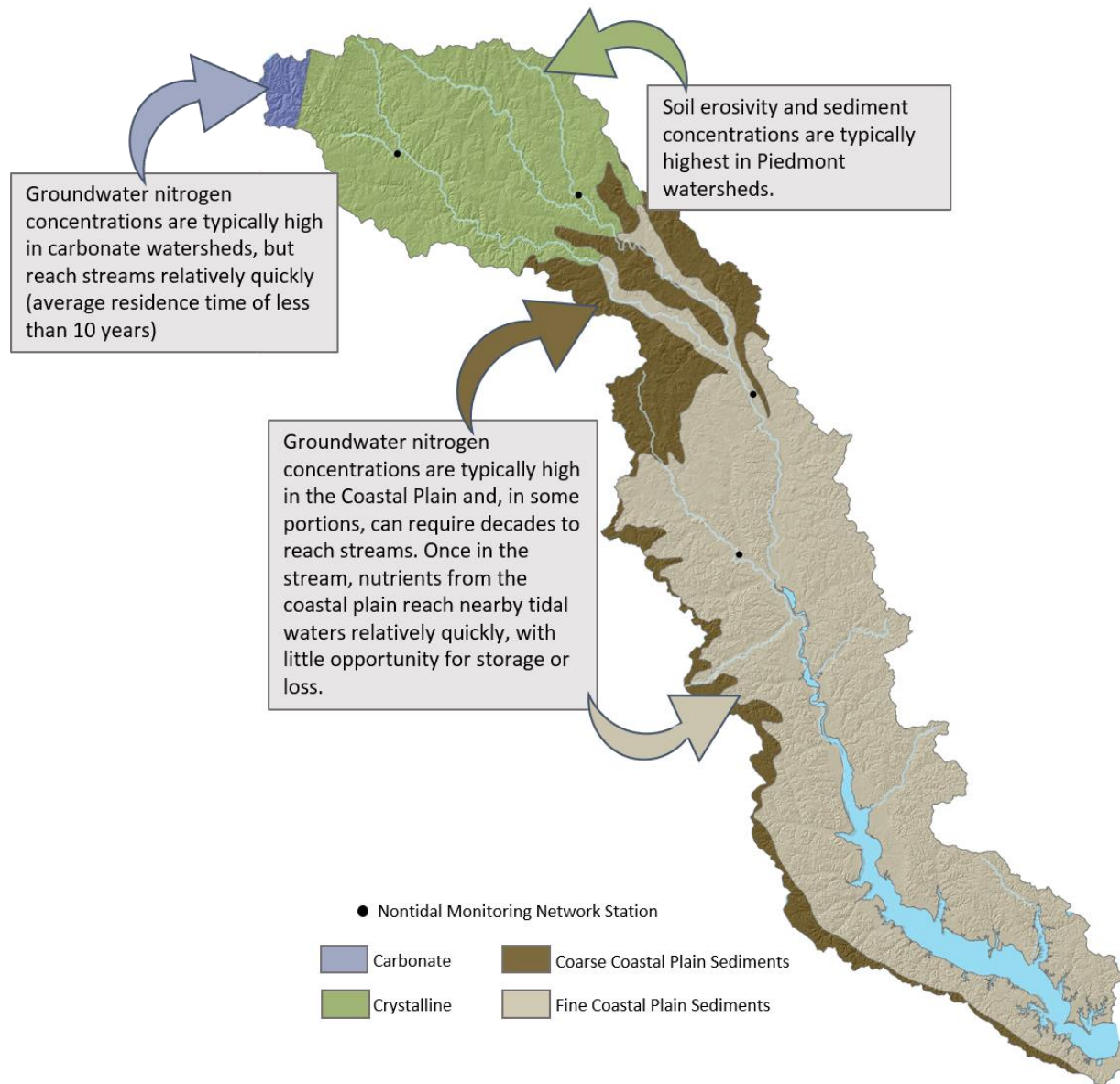


Figure 18. Effects of watershed hydrogeomorphology on nutrient transport to freshwater streams and tidal waters. Base map modified from King *et al.* (1974) and Ator *et al.* (2005), North American Datum 1983.

Nitrogen

Groundwater is an important delivery pathway of nitrogen, as nitrate, to most streams in the Chesapeake Bay watershed (Ator and Denver, 2012; Lizarraga, 1997) and represents about 20 to 75 percent of the total nitrogen load in the Patuxent River watershed (Preston, 1996). Groundwater nitrate concentrations are higher in the Piedmont than in the Coastal Plain section of the Patuxent River watershed (Greene and others, 2005; Terziotti and others, 2017) because Piedmont crystalline rocks contain large amounts of oxidic groundwater, which promote nitrate transport (Tesoriero and others,

2015). In comparison, the Coastal Plain sediments underlying the lower portion of the Patuxent River watershed have geochemical properties that reduce nitrate concentrations in groundwater (Bachman and Krantz, 2000). The typical residence time of groundwater delivered to streams in the Chesapeake Bay watershed is about 10 years, but ages vary from less than one year to greater than 50 years based on bedrock structure, groundwater flow paths, and aquifer depths (Lindsey and others, 2003). The average transit time for nitrate carried through the surficial aquifer in the Maryland Coastal Plain has been estimated to be about 20 years (Focazio and others, 1998) and estimates are much more varied in Piedmont regions (Phillips and others, 1999). Groundwater discharge in the Coastal Plain portion of the Patuxent River watershed can represent greater than 50 percent of total streamflow (Presto and Summers, 1997), with the remaining portion of streamflow is composed of soil moisture and runoff, which have residence times of months to days (Phillips, 2007).

Phosphorus

Phosphorus binds to soil particles and most phosphorus delivered to the Bay is attached to sediment (Zhang *et al.*, 2015); however, once fully phosphorus saturated, soils will not retain new applications and export of dissolved phosphorus to streams, from shallow soils and groundwater, will increase (Staver and Brinsfield, 2001). Phosphorus sorption capacity varies based on soil particle chemical composition and physical structure with clays typically having the greatest number of sorption sites and highest average phosphorus concentrations (Sharpley, 1980). The highest soil phosphorus concentrations in the Patuxent River watershed typically occur in agricultural areas where inputs of manure and fertilizer exceed crop needs. Reducing soil phosphorus concentrations can take a decade or more (Kleinman *et al.*, 2011) and, until this occurs, watershed phosphorus loads may be unresponsive to management practices (Jarvie *et al.*, 2013; Sharpley *et al.*, 2013).

Sediment

The delivery of sediment from upland soil erosion, streambank erosion, and tributary loading varies throughout the Patuxent River watershed, but in-stream concentrations are typically highest in the upper portion of watershed that drains Piedmont geology (Brakebill *et al.*, 2010). The erosivity of Piedmont soils results from its unique topography and from the prevalence of agricultural and urban land uses in these areas (Trimble, 1975; Gellis *et al.*, 2005; Brakebill *et al.*, 2010). Less sediment is mobilized in the Coastal Plain portion of the Patuxent River watershed where stream gradients are lower and floodplains are typically wider (Hupp, 2000). Other factors affecting streambank erosion are highly variable throughout this watershed and include drainage area (Trimble, 1975; Gellis *et al.*, 2005; Brakebill *et al.*, 2010), bank sediment density (Wynn and Mostaghimi, 2006), vegetation (Wynn and Mostaghimi, 2006), stream valley geomorphology (Hopkins *et al.*, 2018), and developed land uses (Brakebill *et al.*, 2010).

Delivery to tidal waters from the non-tidal watershed

The delivery of nitrogen, phosphorus, and sediment in non-tidal streams to tidal waters in the Patuxent River watershed shore varies based on physical and chemical factors that affect in-stream retention, loss, or storage. Less than 25% of all nitrogen and phosphorus inputs to the Patuxent River watershed are estimated to reach the Bay (Boynton *et al.*, 2008). In general, nutrient and sediment loads in tidal waters are most strongly influenced by conditions in proximal non-tidal streams that have less opportunity for denitrification and floodplain trapping of sediment associated phosphorus. There are no

natural chemical processes that remove phosphorus from streams, but sediment, and associated phosphorus, can be trapped in floodplains before reaching tidal waters. High rates of sediment trapping by Coastal Plain nontidal floodplains and head-of-tide tidal freshwater wetlands creates a sediment shadow in many tidal rivers and limits sediment delivery to the bay (Noe and Hupp, 2009; Ensign *et al.*, 2014). Shoreline erosion contributes more fine-grained sediment to estuarine waters in Maryland's western shore than is delivered from the watershed (Langland and Cronin, 2003), likely as a result of such trapping and relatively small upland watershed areas.

5.1.2 Estimated Nutrient and Sediment Loads

Estimated loads to tidal portions of Chesapeake Bay tributaries are a combination of monitored fluxes from U.S. Geological Survey (USGS) River Input Monitoring (RIM) stations located at the nontidal-tidal interface and below-RIM simulated loads from the Chesapeake Bay Program Watershed Model. Nitrogen, phosphorus, and suspended sediment loads to the tidal Patuxent were primarily from the below-RIM areas, although contributions from the RIM areas were also substantial (Figure 19). Over the period of 1985-2018, 0.060, 0.0056, and 5.7 million tons of nitrogen, phosphorus, and suspended sediment loads were exported through the Patuxent River watershed, with 61%, 66%, and 85% of those loads from the below-RIM areas, respectively.

Mann-Kendall trends and Sen's slope estimates are summarized for each loading source in Table 4.

Nitrogen

Estimated TN loads showed an overall decline of 22 ton/yr in the period between 1985 and 2018, which is statistically significant ($p < 0.01$). This reduction reflects a combination of reductions in RIM loads (-14 ton/yr; $p < 0.01$) and below-RIM loads (-9.8 ton/yr; $p < 0.05$). The below-RIM reduction is driven by below-RIM point sources (-6.5 ton/yr, $p < 0.01$), and to a lesser extent, by atmospheric deposition to the tidal waters (-0.90 ton/yr, $p < 0.01$). The below-RIM nonpoint sources also showed a long-term decline (-2.0 ton/yr), although it is not statistically significant ($p = 0.68$). The significant below-RIM point source reductions in TN are a result of substantial efforts to reduce nitrogen loads from several major wastewater treatment facilities by implementing biological nutrient removal (Boynton *et al.*, 2008; Lyerly *et al.*, 2014). The significant decline in atmospheric deposition of TN to the tidal waters is consistent with findings that atmospheric deposition of nitrogen has decreased due to benefits from the Clean Air Act implementation (Eshleman *et al.*, 2013; Lyerly *et al.*, 2014)

Phosphorus

Estimated TP loads showed an overall decline of 0.52 ton/yr in the period between 1985 and 2018, although it is not statistically significant ($p = 0.61$). The RIM loads showed a long-term reduction (-0.41 ton/yr), while the below-RIM loads showed a much smaller long-term decline (-0.030 ton/yr), but both trends are not statistically significant. Within the below-RIM load, point sources showed a statistically significant decline in this period (-0.42 ton/yr; $p < 0.01$), whereas nonpoint sources showed a long-term increase (0.63 ton/yr; $p = 0.33$). This TP point source load reduction has also been attributed to significant efforts to reduce phosphorus in wastewater discharge through the phosphorus detergent ban

in the early part of this record, as well as technology upgrades at wastewater treatment facilities (Boynnton *et al.*, 2008; Lyerly *et al.*, 2014).

Sediment

Estimated suspended sediment (SS) loads showed an overall increase of 1,477 ton/yr in the period between 1985 and 2018, although it is not statistically significant ($p = 0.06$). Both the RIM and below-RIM loads showed long-term increases, but both are not statistically significant. Notably, the below-RIM increase is almost entirely attributable to nonpoint sources (1,040 ton/yr; $p = 0.05$).

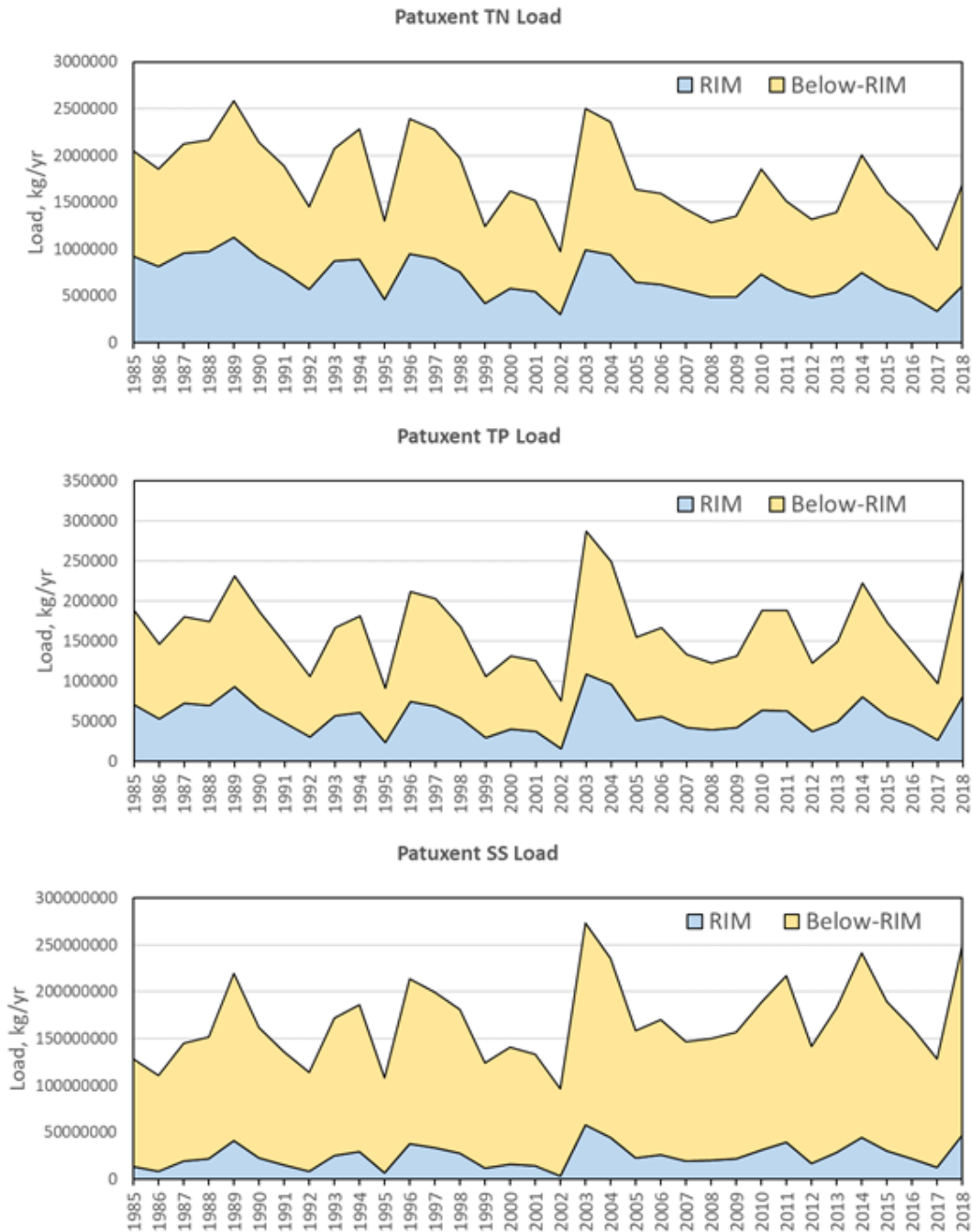


Figure 19. Estimated total loads of nitrogen (TN), phosphorus (TP), and suspended sediment (SS) from the RIM and below-RIM areas of the Patuxent River. RIM refers to the USGS River Input Monitoring site located just above the head of tide of this tributary, which includes upstream point source loads. Below-RIM estimates are a combination of simulated non-point source, atmospheric deposition, and reported point-source loads.

Table 4. Summary of Mann-Kendall trends for the period of 1985-2018 for total nitrogen (TN), total phosphorus (TP), and suspended sediment (SS) loads from the Patuxent River watershed.

Variable	Trend, metric ton/yr	Trend p-value
TN		
<i>Total watershed</i>	-22	< 0.01
<i>RIM watershed</i> ¹	-14	< 0.01
<i>Below-RIM watershed</i> ²	-9.8	< 0.05
<i>Below-RIM point source</i>	-6.5	< 0.01
<i>Below-RIM nonpoint source</i> ³	-2.0	0.68
<i>Below-RIM tidal deposition</i>	-0.90	< 0.01
TP		
<i>Total watershed</i>	-0.52	0.61
<i>RIM watershed</i>	-0.41	0.29
<i>Below-RIM watershed</i>	-0.030	0.98
<i>Below-RIM point source</i>	-0.42	< 0.01
<i>Below-RIM nonpoint source</i>	0.63	0.33
SS		
<i>Total watershed</i>	1,477	0.06
<i>RIM watershed</i>	396	0.07
<i>Below-RIM watershed</i>	1,041	0.05
<i>Below-RIM point source</i>	0.57	< 0.01
<i>Below-RIM nonpoint source</i>	1,040	0.05

¹ Loads for the RIM watershed were estimated loads at the USGS RIM station 01594440 (Patuxent River near Bowie, Md.; https://cbrim.er.usgs.gov/loads_query.html).

² Loads for the below-RIM watershed were obtained from the Chesapeake Bay Program Watershed Model (<https://cast.chesapeakebay.net/>).

³ Below-RIM nonpoint source loads were obtained from the Chesapeake Bay Program Watershed Model's progress runs specific to each year from 1985 and 2018, which were adjusted to reflect actual hydrology using the method of the Chesapeake Bay Program's Loads to the Bay indicator (see <https://www.chesapeakeprogress.com/clean-water/water-quality>).

5.1.3 Expected Effects of Changing Watershed Conditions

According to the Chesapeake Bay Program's Watershed Model known as the Chesapeake Assessment Scenario Tool (CAST; <https://cast.chesapeakebay.net>, version CAST-2019), changes in population size, land use, and pollution management controls between 1985 and 2019 would be expected to change long-term average nitrogen, phosphorus, and sediment loads to the tidal Patuxent River by -32%, -55%, and -10%, respectively (Figure 20). In contrast to the annual loads analysis above, CAST loads are based on changes in management only and do not include annual fluctuations in weather. CAST loads are calculated without lag times for delivery of pollutants or lags related to BMPs becoming fully effective after installation. In 1985, wastewater and agriculture were the two largest sources of nitrogen loads. By

2019, wastewater nitrogen loads had changed by -80% and developed sector was now the largest nitrogen source. The agriculture sector remained the second largest nitrogen source. Overall, decreasing nitrogen loads from agriculture (-49%), natural (-13%), stream bed and bank (-17%), and wastewater (-80%) sources were partially counteracted by increases from developed (58%) and septic (93%) sources.

The two largest sources of phosphorus loads as of 2019 were the developed and stream bed and bank sectors. Overall, expected declines from agriculture (-71%), natural (-20%), stream bed and bank (-48%), and wastewater (-86%) sources were partially counteracted by increases from developed (21%) sources.

For sediment, the largest sources are shoreline and stream bed and bank areas: these two sources changed by -1% and -12%, respectively between 1985 and 2019. Sediment loads from the agriculture sector changed by -67%, whereas sediment load from developed areas changed by 47%.

Overall, changing watershed conditions are expected to result in the agriculture, natural, and stream bed and bank sectors achieving reductions in nitrogen, phosphorus, and sediment loads between 1985 and 2019, whereas the developed and non-tidal water atmospheric deposition sectors are expected to increase in nitrogen, phosphorus, and sediment loads.

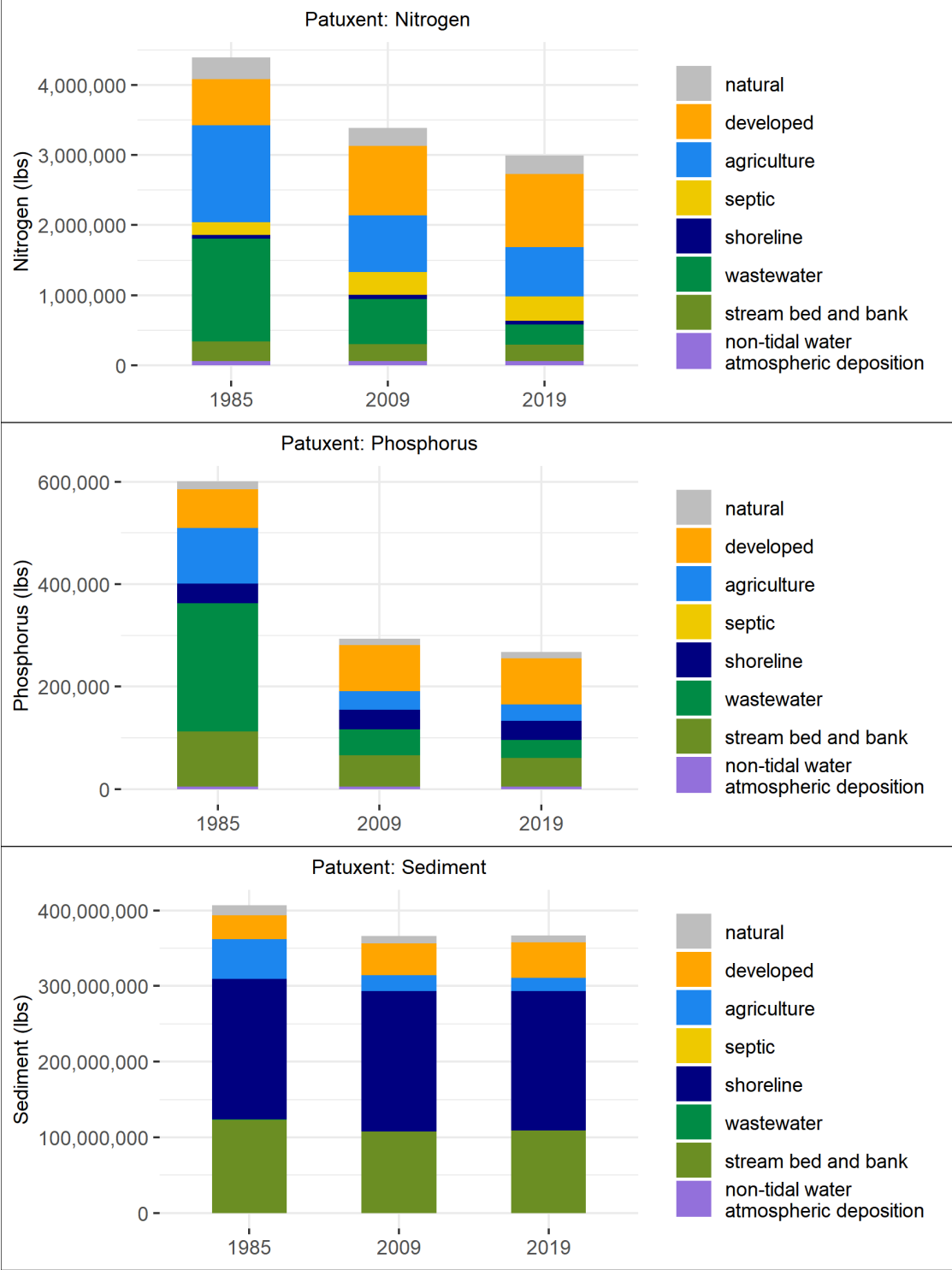
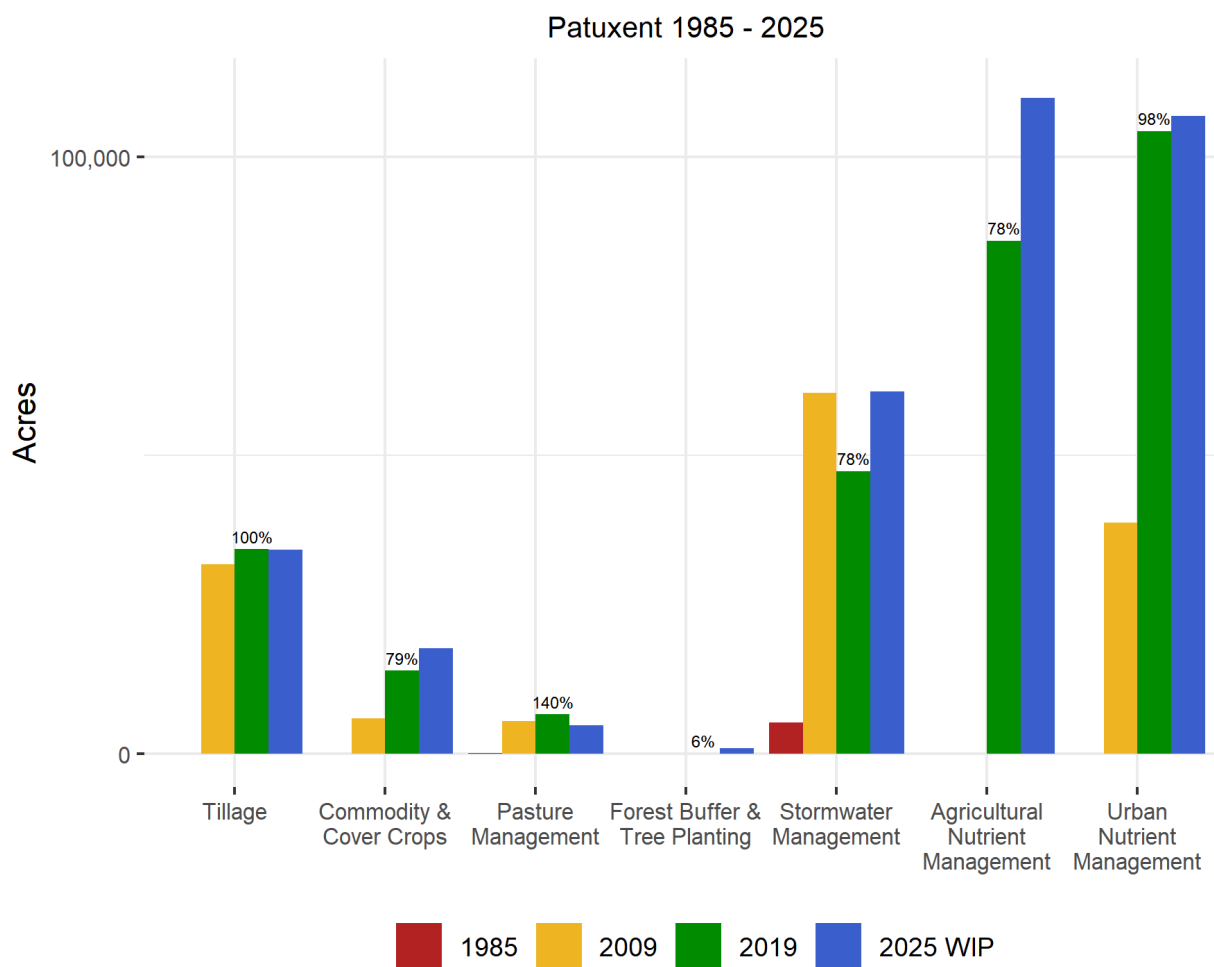


Figure 20. Expected long-term average loads of nitrogen, phosphorus, and sediment from different sources to the tidal Patuxent, as obtained from the Chesapeake Assessment Scenario Tool (CAST). Data shown are time-average delivered loads over the average hydrology of 1991-2000, once the steady state is reached for the conditions on the ground, as obtained from the 1985, 2009, and 2019 progress (management) scenarios.

5.1.4 Best Management Practices (BMPs) Implementation

Data on reported BMP implementation are available for download from CAST (<https://cast.chesapeakebay.net>, version CAST-2019). Reported BMP implementations on the ground as of 1985, 2009, and 2019 are compared to planned 2025 implementation levels in Figure 21 for a subset of major BMP groups measured in acres. As of 2019, tillage, cover crops, pasture management, forest buffer and tree planting, stormwater management, agricultural nutrient management, and urban nutrient management were credited for 34, 14, 7, 0.1, 47, 86, and 104 thousand acres, respectively. Implementation levels for some practices are already close to achieving their planned 2025 levels: for example, 140% of planned acres for pasture management had been achieved as of 2019. In contrast, about 78% of planned stormwater management implementation had been achieved as of 2019.



Values above the 2019 bars are the percent of the 2025 goal achieved.

Figure 21. BMP implementation in the Patuxent watershed

Stream restoration and animal waste management system systems are two important BMPs that cannot be compared directly with those above because they are measured in different units. However, progress towards implementation goals can still be documented. Stream restoration (agricultural and urban) had increased from 0 feet in 1985 to 41,621 feet in 2019. Over the same period, animal waste management

systems treated 0 animal units in 1985 and 1,082 animal units in 2019 (one animal unit represents 1,000 pounds of live animal). These implementation levels represent 17% and 8% of their planned 2025 implementation levels, respectively.

5.1.5 Flow-Normalized Watershed Nutrient and Sediment Loads

Flow normalization can better reveal temporal trends in river water quality by removing the effect of inter-annual variability in streamflow. Flow-normalized trends help scientists evaluate changes in load resulting from changing sources, delays associated with storage or transport of historical inputs, and/or implemented management actions. Flow-normalized nitrogen, phosphorus, and sediment trends have been reported for the long term (1985-2019) and short term (2009-2018) at nontidal network stations throughout the watershed (Moyer and Langland, 2020) (Table 5). These trends result from variability in nutrient applications, the delivery of nutrients and sediment from the landscape to streams, and from processes that affect in-stream loss or retention of nutrients and sediment.

Table 5. Long-term (1985 - 2018) and short-term trends (2009 - 2018) of flow-normalized total nitrogen (TN), total phosphorus (TP), and suspended sediment (SS) loads for nontidal network monitoring locations in the Patuxent River watershed. A more detailed summary of flow-normalized loads and trends measured at all USGS Chesapeake Bay Nontidal Network stations can be found at <https://cbrim.er.usgs.gov/summary.html>.

USGS Station ID	USGS Station Name	Trend start water year	Percent change in FN load, through water year 2018		
			TN	TP	SS
01591000	PATUXENT RIVER NEAR UNITY, MD	1985	2.7	-58.6	-1.3
		2009	7.5	18.5	19.4
01594440	PATUXEN RIVER AT BOWIE, MD	1985	-65.4	-64.2	-39.8
		2009	-20.7	-6.4	1.2
01594526	WESTERN BRANCH AT UPPER MARLBORO, MD	2009	-6.3	-10.4	-9.9

Decreasing trends listed in green, increasing trends listed in orange, results reported as "no trend" listed in black. TN = total nitrogen, TP = total phosphorus, SS = suspended sediment

5.2 Tidal Factors

Once pollutants reach tidal waters, a complex set of environmental factors interact with them to affect key habitat indicators like algal biomass, DO concentrations, water clarity, submerged aquatic vegetation (SAV) abundance, and fish populations (Kemp *et al.*, 2005; Testa *et al.*, 2017) (Figure 22). For example, phytoplankton growth depends not just on nitrogen and phosphorus (Fisher *et al.*, 1992; Kemp *et al.*, 2005; Zhang *et al.*, 2021), but also on light and water temperature (Buchanan *et al.*, 2005; Buchanan, 2020). In general, the saline waters of the lower Bay tend to be more transparent than tidal-fresh regions, and waters adjacent to nutrient input points are more affected by these inputs than more distant regions (Keisman *et al.*, 2019; Testa *et al.*, 2019). Dissolved oxygen concentrations are affected by salinity- and temperature-driven stratification of the water column, and conversely by wind-driven mixing, in addition to phytoplankton respiration and decomposition (Scully, 2010; Murphy *et al.*, 2011). When anoxia occurs at the water-sediment interface, nitrogen and phosphorus stored in the sediments

can be released through anaerobic chemical reactions (Testa and Kemp, 2012). When low-oxygen water and sediment burial suffocate benthic plant and animal communities, their nutrient consumption and water filtration services are lost. Conversely, when conditions improve enough to support abundant SAV and benthic communities, their functions can sustain and even advance progress towards a healthier ecosystem (Cloern, 1982; Phelps, 1994; Ruhl and Rybicki, 2010; Gurbisz and Kemp, 2014).

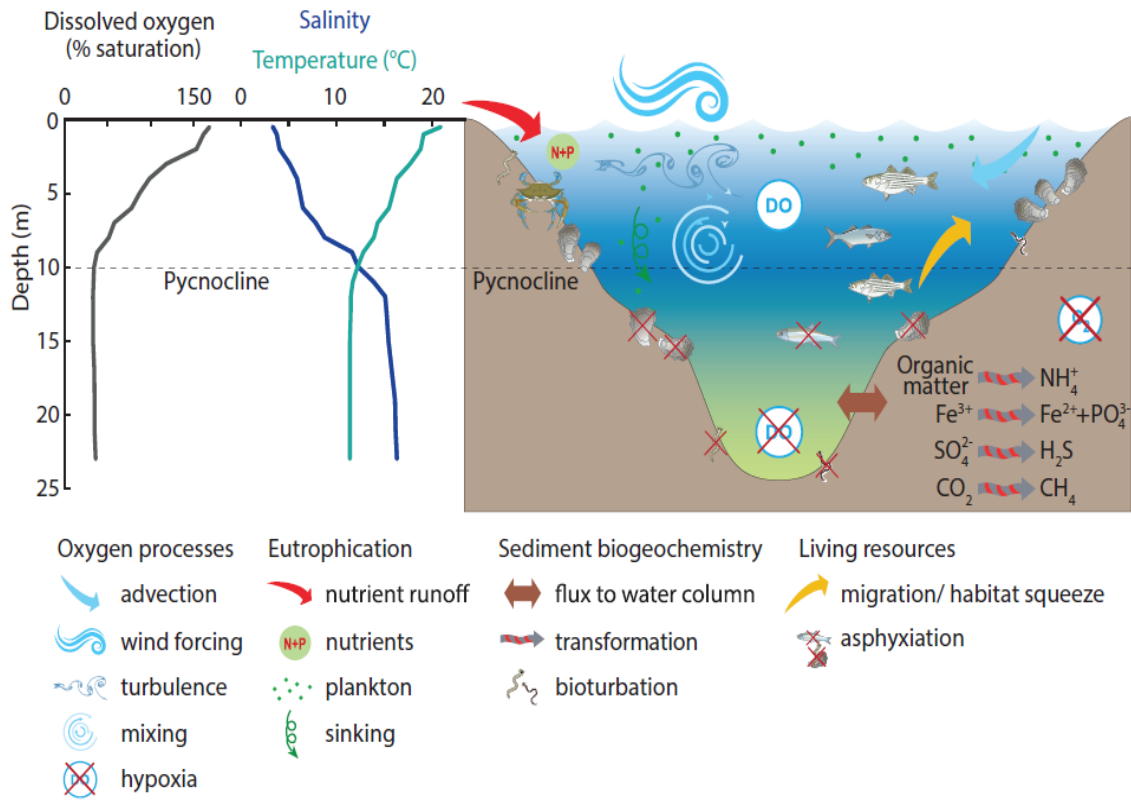


Figure 22. Conceptual diagram illustrating how hypoxia is driven by eutrophication and physical forcing, while affecting sediment biogeochemistry and living resources. From Testa *et al.* (2017).

High nutrient loads relative to tidal river size are indicative of areas that are more susceptible to eutrophication (Bricker *et al.*, 2003; Ferreira *et al.*, 2007). The relationship between watershed area and tidal river size may also be an important indicator of eutrophication potential, however there are competing effects. A large watershed relative to the volume of receiving water would likely correlate with higher nutrient loads, however it would also correlate with a higher flow rate and decreased flushing time (Bricker *et al.*, 2008). Figure 23 is a comparison of watershed area versus estuarine volume for all estuaries and sub-estuaries identified in the CBP monitoring segment scheme. Larger estuaries will contain multiple monitoring segments and, in many cases, sub-estuaries. For example, the Potomac River contains monitoring segments in the tidal fresh, oligohaline, and mesohaline sections of the river as well as the entire Anacostia River and other sub-estuaries. Figures 24 and 25 are comparisons of estimated annual average nitrogen and phosphorus loads, respectively, for the 2018 progress scenario in CAST versus the estuarine volume for the same set of estuaries and sub-estuaries.

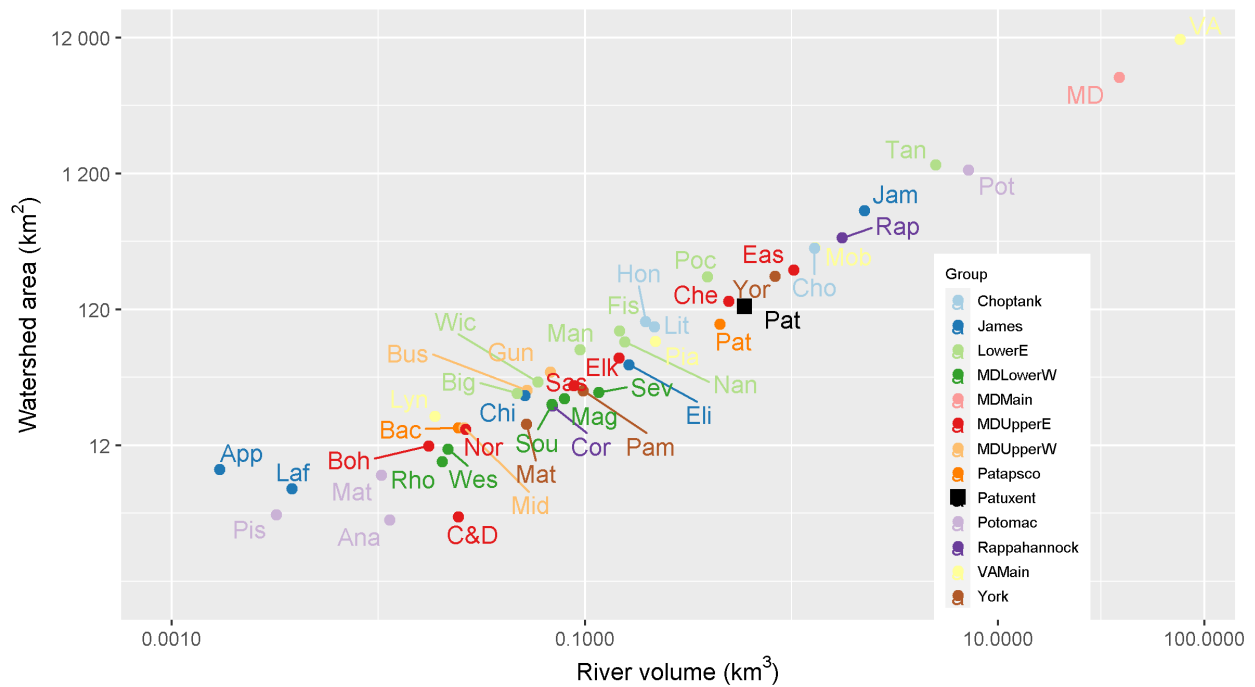


Figure 23. Watershed area vs estuarine volume.

<u>Abbreviated tributary name</u>	<u>Full tributary name</u>	<u>Abbreviated tributary name</u>	<u>Full tributary name</u>
Ana	Anacostia River	Mat	Mattaponi River
App	Appomattox River	MD	MD MAINSTEM
Bac	Back River	Mid	Middle River
Big	Big Annemessex River	Mob	Mobjack Bay
Boh	Bohemia River	Nan	Nanticoke River
Bus	Bush River	Nor	Northeast River
C&D	C&D Canal	Pam	Pamunkey River
Che	Chester River	Pat	Patapsco River
Chi	Chickahominy River	Pat	Patuxent River
Cho	Choptank River	Pia	Piankatank River
Cor	Corrotoman River	Pis	Piscataway Creek
Eas	Eastern Bay	Poc	Pocomoke River
Eli	Elizabeth River	Pot	Potomac River
Elk	Elk River	Rap	Rappahannock River
Fis	Fishing Bay	Rho	Rhode River
Gun	Gunpowder River	Sas	Sassafras River
Hon	Honga River	Sev	Severn River
Jam	James River	Sou	South River
Laf	Lafayette River	Tan	Tangier Sound
Lit	Little Choptank River	VA	VA MAINSTEM
Lyn	Lynnhaven River	Wes	West River
Mag	Magothy River	Wes	Western Branch (Patuxent River)
Man	Manokin River	Wic	Wicomico River
Mat	Mattawoman Creek	Yor	York River

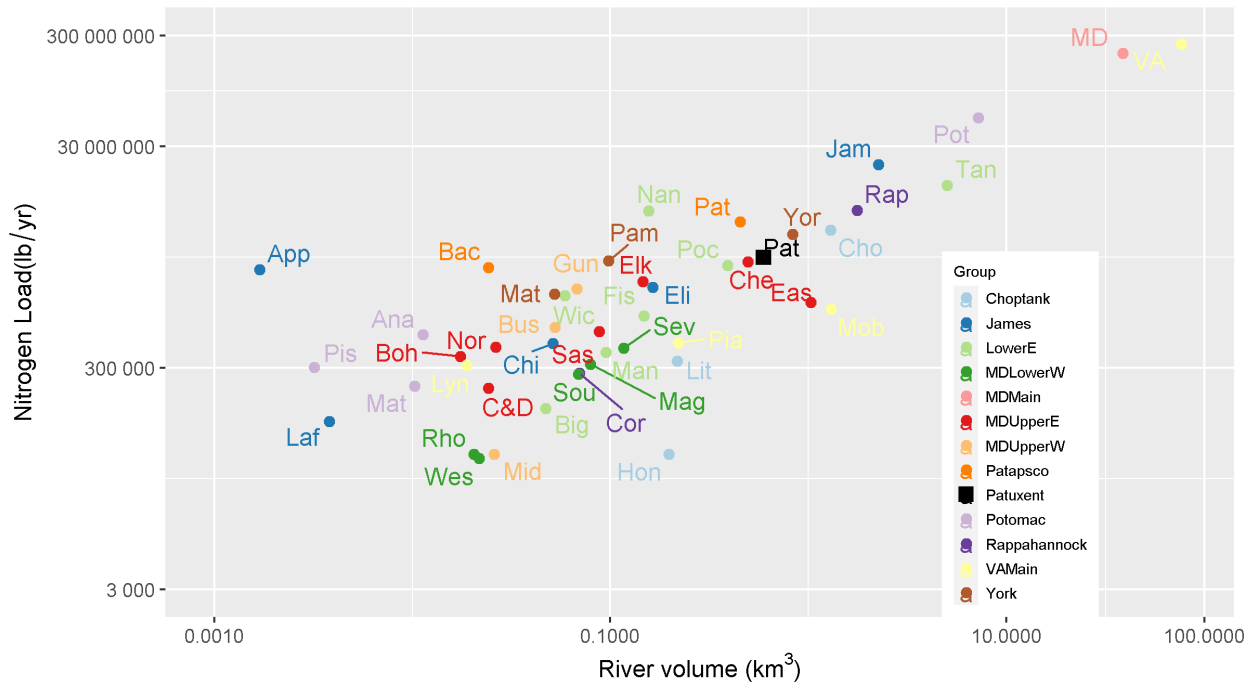


Figure 24. Annual average expected nitrogen loads versus estuarine volume. Nitrogen loads are from the 2018 progress scenarios in CAST (Chesapeake Bay Program, 2020), which is an estimate of nitrogen loads under long-term average hydrology given land use and reported management as of 2018.

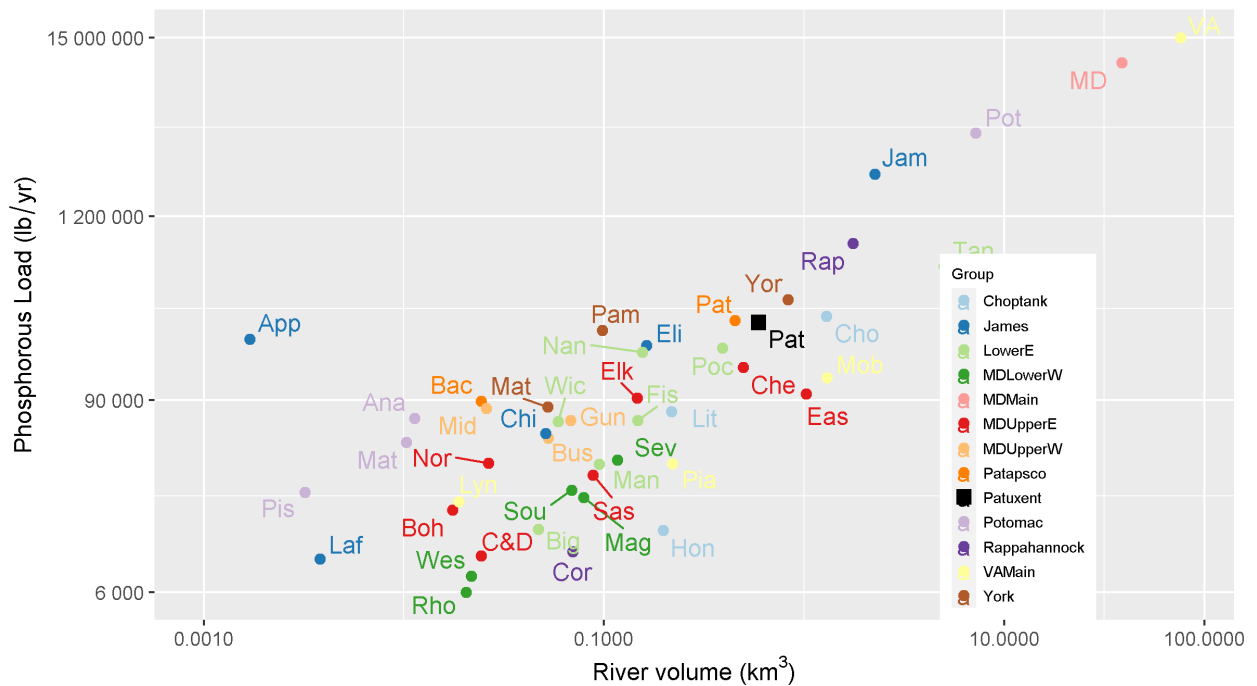


Figure 25. Annual average expected phosphorus loads versus estuarine volume. Phosphorus loads are from the 2018 progress scenarios in CAST (Chesapeake Bay Program, 2020), which is an estimate of

phosphorus loads under long-term average hydrology given land use and reported management as of 2018.

The Patuxent river estuary volume and watershed contain approximately 0.8 and 1% of the total volume and watershed of the Chesapeake Bay. This ranks the Patuxent as the 10th largest volume and 8th largest watershed area aggregated tributary in this summary (Figures 23, 24, and 25). The ratios of watershed area, nitrogen loading, and phosphorus loading to estuarine volume are consistent with other estuaries in the Chesapeake system, indicating a moderate level of susceptibility to eutrophication.

5.3 Insights on Changes in the Patuxent

Completion of Section 5.3 is contingent upon stakeholder interest and availability of resources.

It requires:

- *Synthesis of the information provided in previous sections and of the recent literature on explaining trends in general and any work conducted on this tributary in particular;*
- *Discussion with local technical experts to clarify insights and vet hypotheses and preliminary findings.*

6. Summary

Completion of Section 6 is contingent upon completion of Section 5.3.

References

- Ator, S. W., J. D. Blomquist, J. S. Webber and J. G. Chanat, 2020. Factors driving nutrient trends in streams of the Chesapeake Bay watershed. *J. Environ. Qual.* 49:812-834, DOI: 10.1002/jeq2.20101.
- Ator, S. W., J. W. Brakebill and J. D. Blomquist, 2011. Sources, fate, and transport of nitrogen and phosphorus in the Chesapeake Bay watershed: An empirical model. U.S. Geological Survey Scientific Investigations Report 2011-5167, Reston, VA, p. 27. <http://pubs.usgs.gov/sir/2011/5167/>.
- Ator, S. W., J. M. Denver, D. E. Krantz, W. L. Newell and S. K. Martucci, 2005. A Surficial Hydrogeologic Framework for the Mid-Atlantic Coastal Plain. U.S. Geological Survey U.S. Geological Survey Professional Paper 1680. <https://pubs.usgs.gov/pp/2005/pp1680/>.
- Ator, S. W., A. M. García, G. E. Schwarz, J. D. Blomquist and A. J. Sekellick, 2019. Toward explaining nitrogen and phosphorus trends in Chesapeake Bay tributaries, 1992–2012. *J. Am. Water Resour. Assoc.* 55:1149-1168, DOI: 10.1111/1752-1688.12756.
- Bachman, L. J., B. Lindsey, J. Brakebill and D. S. Powars, 1998. Ground-water discharge and base-flow nitrate loads of nontidal streams, and their relation to a hydrogeomorphic classification of the Chesapeake Bay Watershed, middle Atlantic coast. US Geological Survey Water-Resources Investigations Report 98-4059, Baltimore, MD, p. 71. <http://pubs.usgs.gov/wri/wri98-4059/>.
- Boynton, W. R., J. D. Hagy, J. C. Cornwell, W. M. Kemp, S. M. Greene, M. S. Owens, J. E. Baker and R. K. Larsen, 2008. Nutrient budgets and management actions in the Patuxent River Estuary, Maryland. *Estuaries Coasts* 31:623-651, DOI: 10.1007/s12237-008-9052-9.
- Brakebill, J. W., S. W. Ator and G. E. Schwarz, 2010. Sources of suspended-sediment flux in streams of the Chesapeake Bay watershed: A regional application of the SPARROW Model. *J. Am. Water Resour. Assoc.* 46:757-776, DOI: 10.1111/j.1752-1688.2010.00450.x.
- Bricker, S. B., J. G. Ferreira and T. Simas, 2003. An integrated methodology for assessment of estuarine trophic status. *Ecol. Model.* 169:39-60, DOI: 10.1016/s0304-3800(03)00199-6.
- Bricker, S. B., B. Longstaff, W. Dennison, A. Jones, K. Boicourt, C. Wicks and J. Woerner, 2008. Effects of nutrient enrichment in the nation's estuaries: A decade of change. *Harmful Algae* 8:21-32, DOI: 10.1016/j.hal.2008.08.028.
- Buchanan, C., 2020. A water quality binning method to infer phytoplankton community structure and function. *Estuaries Coasts* 43:661-679, DOI: 10.1007/s12237-020-00714-3.
- Buchanan, C., R. V. Lacouture, H. G. Marshall, M. Olson and J. M. Johnson, 2005. Phytoplankton reference communities for Chesapeake Bay and its tidal tributaries. *Estuaries* 28:138-159, DOI: 10.1007/bf02732760.
- Chesapeake Bay Program, 2018. Data Hub.
- Chesapeake Bay Program, 2020. Chesapeake Assessment and Scenario Tool (CAST) Version 2019.
- Cloern, J. E., 1982. Does the benthos control phytoplankton biomass in South San Francisco Bay? *Mar. Ecol. Prog. Ser.* 9:191-202, DOI: 10.3354/meps009191.
- Ensign, S. H., C. R. Hupp, G. B. Noe, K. W. Krauss and C. L. Stagg, 2014. Sediment accretion in tidal freshwater forests and oligohaline marshes of the Waccamaw and Savannah Rivers, USA. *Estuaries Coasts* 37:1107-1119, DOI: 10.1007/s12237-013-9744-7.
- Eshleman, K. N., R. D. Sabo and K. M. Kline, 2013. Surface water quality is improving due to declining atmospheric N deposition. *Environ. Sci. Technol.* 47:12193-12200, DOI: 10.1021/es4028748.
- Falcone, J. A., 2015. U.S. conterminous wall-to-wall anthropogenic land use trends (NWALT), 1974–2012. U.S. Geological Survey Data Series 948, Reston, VA. <https://doi.org/10.3133/ds948>.

- Ferreira, J. G., S. B. Bricker and T. C. Simas, 2007. Application and sensitivity testing of a eutrophication assessment method on coastal systems in the United States and European Union. *J. Environ. Manage.* 82:433-445, DOI: 10.1016/j.jenvman.2006.01.003.
- Fisher, T. R., E. R. Peele, J. W. Ammerman and L. W. Harding, 1992. Nutrient limitation of phytoplankton in Chesapeake Bay. *Mar. Ecol. Prog. Ser.* 82:51-63, DOI: 10.3354/meps082051.
- Gellis, A. C., W. S. L. Banks, M. J. Langland and S. K. Martucci, 2005. Summary of suspended-sediment data for streams draining the Chesapeake Bay Watershed, water years 1952-2002. US Geological Survey Scientific Investigations Report 2004-5056, Reston, VA, p. 59. <https://doi.org/10.3133/sir20045056>.
- Gurbisz, C. and W. M. Kemp, 2014. Unexpected resurgence of a large submersed plant bed in Chesapeake Bay: Analysis of time series data. *Limnol. Oceanogr.* 59:482-494, DOI: 10.4319/lo.2014.59.2.0482.
- Harding, J. L. W. and E. S. Perry, 1997. Long-term increase of phytoplankton biomass in Chesapeake Bay, 1950-1994. *Mar. Ecol. Prog. Ser.* 157:39-52, DOI: 10.3354/meps157039.
- Hernandez Cordero, A. L., P. J. Tango and R. A. Batiuk, 2020. Development of a multimetric water quality indicator for tracking progress towards the achievement of Chesapeake Bay water quality standards. *Environ. Monit. Assess.* 192:94, DOI: 10.1007/s10661-019-7969-z.
- Hopkins, K. G., G. B. Noe, F. Franco, E. J. Pindilli, S. Gordon, M. J. Metes, P. R. Claggett, A. C. Gellis, C. R. Hupp and D. M. Hogan, 2018. A method to quantify and value floodplain sediment and nutrient retention ecosystem services. *J. Environ. Manage.* 220:65-76, DOI: 10.1016/j.jenvman.2018.05.013.
- Hupp, C. R., 2000. Hydrology, geomorphology and vegetation of Coastal Plain rivers in the south-eastern USA. *Hydrol. Process.* 14:2991-3010, DOI: 10.1002/1099-1085(200011/12)14:16/17%3C2991::AID-HYP131%3E3.0.CO;2-H.
- Jarvie, H. P., A. N. Sharpley, B. Spears, A. R. Buda, L. May and P. J. Kleinman, 2013. Water quality remediation faces unprecedented challenges from "legacy phosphorus". *Environ. Sci. Technol.* 47:8997-8998, DOI: 10.1021/es403160a.
- Keisman, J., C. Friedrichs, R. Batiuk, J. Blomquist, J. Cornwell, C. Gallegos, S. Lyubchich, K. Moore, R. Murphy, R. Orth, L. Sanford, P. Tango, J. Testa, M. Trice and Q. Zhang, 2019. Understanding and explaining 30 years of water clarity trends in the Chesapeake Bay's tidal waters. Chesapeake Bay Program Scientific and Technical Advisory Committee STAC Publication Number 19-004, Edgewater, MD, p. 25. http://www.chesapeake.org/pubs/411_Keisman2019.pdf.
- Kemp, W. M., W. R. Boynton, J. E. Adolf, D. F. Boesch, W. C. Boicourt, G. Brush, J. C. Cornwell, T. R. Fisher, P. M. Glibert, J. D. Hagy, L. W. Harding, E. D. Houde, D. G. Kimmel, W. D. Miller, R. I. E. Newell, M. R. Roman, E. M. Smith and J. C. Stevenson, 2005. Eutrophication of Chesapeake Bay: Historical trends and ecological interactions. *Mar. Ecol. Prog. Ser.* 303:1-29, DOI: 10.3354/meps303001.
- King, P. B., H. M. Beikman and G. J. Edmonston, 1974. Geologic map of the United States (exclusive of Alaska and Hawaii). U.S. Geological Survey. <https://doi.org/10.3133/70136641>.
- Kleinman, P., A. Sharpley, A. Buda, R. McDowell and A. Allen, 2011. Soil controls of phosphorus in runoff: Management barriers and opportunities. *Can. J. Soil Sci.* 91:329-338, DOI: 10.4141/cjss09106.
- Langland, M. J. and T. Cronin, 2003. A summary report of sediment processes in Chesapeake Bay and watershed. US Geological Survey Water-Resources Investigations Report 03-4123, New Cumberland, PA, p. 109. pa.water.usgs.gov/reports/wrir03-4123.pdf.
- Lyerly, C. M., A. L. H. Cordero, K. L. Foreman, S. W. Phillips and W. C. Dennison, 2014. New insights: Science-based evidence of water quality improvements, challenges, and opportunities in the Chesapeake. Annapolis, MD, p. 47. http://ian.umces.edu/pdfs/ian_report_438.pdf.

- Moyer, D. L. and M. J. Langland, 2020. Nitrogen, phosphorus, and suspended-sediment loads and trends measured at the Chesapeake Bay Nontidal Network stations: Water years 1985-2018. Accessed <https://doi.org/10.5066/P931M7FT>.
- Murphy, R. R., W. M. Kemp and W. P. Ball, 2011. Long-term trends in Chesapeake Bay seasonal hypoxia, stratification, and nutrient loading. *Estuaries Coasts* 34:1293-1309, DOI: 10.1007/s12237-011-9413-7.
- Murphy, R. R., E. Perry, J. Harcum and J. Keisman, 2019. A generalized additive model approach to evaluating water quality: Chesapeake Bay case study. *Environ. Model. Software* 118:1-13, DOI: 10.1016/j.envsoft.2019.03.027.
- Noe, G. B., M. J. Cashman, K. Skalak, A. Gellis, K. G. Hopkins, D. Moyer, J. Webber, A. Benthem, K. Maloney, J. Brakebill, A. Sekellick, M. Langland, Q. Zhang, G. Shenk, J. Keisman and C. Hupp, 2020. Sediment dynamics and implications for management: State of the science from long-term research in the Chesapeake Bay watershed, USA. *Wiley Interdisciplinary Reviews: Water* 7:e1454, DOI: 10.1002/wat2.1454.
- Noe, G. B. and C. R. Hupp, 2009. Retention of riverine sediment and nutrient loads by coastal plain floodplains. *Ecosystems* 12:728-746, DOI: 10.1007/s10021-009-9253-5.
- Phelps, H. L., 1994. The asiatic clam (*Corbicula fluminea*) invasion and system-level ecological change in the Potomac River Estuary near Washington, D.C. *Estuaries* 17:614-621, DOI: 10.2307/1352409.
- Ruhl, H. A. and N. B. Rybicki, 2010. Long-term reductions in anthropogenic nutrients link to improvements in Chesapeake Bay habitat. *Proc. Natl. Acad. Sci. U. S. A.* 107:16566-16570, DOI: 10.1073/pnas.1003590107.
- Scully, M. E., 2010. Wind modulation of dissolved oxygen in Chesapeake Bay. *Estuaries Coasts* 33:1164-1175, DOI: 10.1007/s12237-010-9319-9.
- Sharpley, A., H. P. Jarvie, A. Buda, L. May, B. Spears and P. Kleinman, 2013. Phosphorus legacy: Overcoming the effects of past management practices to mitigate future water quality impairment. *J. Environ. Qual.* 42:1308-1326, DOI: 10.2134/jeq2013.03.0098.
- Sharpley, A. N., 1980. The enrichment of soil phosphorus in runoff sediments. *J. Environ. Qual.* 9:521-526, DOI: 10.2134/jeq1980.00472425000900030039x.
- Smith, E. M. and W. M. Kemp, 1995. Seasonal and regional variations in plankton community production and respiration for Chesapeake Bay. *Mar. Ecol. Prog. Ser.* 116:217-231, DOI.
- Staver, K. W. and R. B. Brinsfield, 2001. Agriculture and water quality on the Maryland eastern shore: Where do we go from here? *Bioscience* 51:859-868, DOI: 10.1641/0006-3568(2001)051[0859:Aawqot]2.0.Co;2.
- Tango, P. J. and R. A. Batiuk, 2013. Deriving Chesapeake Bay water quality standards. *J. Am. Water Resour. Assoc.* 49:1007-1024, DOI: 10.1111/jawr.12108.
- Testa, J. M., J. B. Clark, W. C. Dennison, E. C. Donovan, A. W. Fisher, W. Ni, M. Parker, D. Scavia, S. E. Spitzer, A. M. Waldrop, V. M. D. Vargas and G. Ziegler, 2017. Ecological forecasting and the science of hypoxia in Chesapeake Bay. *Bioscience* 67:614-626, DOI: 10.1093/biosci/bix048.
- Testa, J. M. and W. M. Kemp, 2012. Hypoxia-induced shifts in nitrogen and phosphorus cycling in Chesapeake Bay. *Limnol. Oceanogr.* 57:835-850, DOI: 10.4319/lo.2012.57.3.0835.
- Testa, J. M., V. Lyubchich and Q. Zhang, 2019. Patterns and trends in Secchi disk depth over three decades in the Chesapeake Bay estuarine complex. *Estuaries Coasts* 42:927-943, DOI: 10.1007/s12237-019-00547-9.
- Trimble, S. W., 1975. A volumetric estimate of man-induced soil erosion on the southern Piedmont Plateau. Agricultural Research Service, U.S. Department of Agriculture Agricultural Research Service Publication ARS-S-40, pp. 142-154.

- U.S. Environmental Protection Agency, 2003. Ambient water quality criteria for dissolved oxygen, water clarity and chlorophyll-a for the Chesapeake Bay and its tidal tributaries. USEPA Region III Chesapeake Bay Program Office EPA 903-R-03-002, Annapolis, Maryland.
- U.S. Environmental Protection Agency, 2004. Chesapeake Bay Program analytical segmentation scheme: Revisions, decisions and rationales 1983-2003. USEPA Region III Chesapeake Bay Program Office EPA 903-R-04-008, Annapolis, Maryland, p. 64.
- Wynn, T. and S. Mostaghimi, 2006. The effects of vegetation and soil type on streambank erosion, southwestern Virginia, USA. *J. Am. Water Resour. Assoc.* 42:69-82, DOI: 10.1111/j.1752-1688.2006.tb03824.x.
- Zhang, Q., D. C. Brady, W. R. Boynton and W. P. Ball, 2015. Long-term trends of nutrients and sediment from the nontidal Chesapeake watershed: An assessment of progress by river and season. *J. Am. Water Resour. Assoc.* 51:1534-1555, DOI: 10.1111/1752-1688.12327.
- Zhang, Q., T. R. Fisher, E. M. Trentacoste, C. Buchanan, A. B. Gustafson, R. Karrh, R. R. Murphy, J. Keisman, C. Wu, R. Tian, J. M. Testa and P. J. Tango, 2021. Nutrient limitation of phytoplankton in Chesapeake Bay: Development of an empirical approach for water-quality management. *Water Res.* 188:116407, DOI: 10.1016/j.watres.2020.116407.
- Zhang, Q., R. R. Murphy, R. Tian, M. K. Forsyth, E. M. Trentacoste, J. Keisman and P. J. Tango, 2018a. Chesapeake Bay's water quality condition has been recovering: Insights from a multimetric indicator assessment of thirty years of tidal monitoring data. *Sci. Total Environ.* 637-638:1617-1625, DOI: 10.1016/j.scitotenv.2018.05.025.
- Zhang, Q., P. J. Tango, R. R. Murphy, M. K. Forsyth, R. Tian, J. Keisman and E. M. Trentacoste, 2018b. Chesapeake Bay dissolved oxygen criterion attainment deficit: Three decades of temporal and spatial patterns. *Frontiers in Marine Science* 5:422, DOI: 10.3389/fmars.2018.00422.

Appendix

Additional tidal trend maps and plots are in a separate Appendix document for:

- Bottom Total Nitrogen
- Bottom Total Phosphorus
- Surface Dissolved Inorganic Nitrogen
- Surface Orthophosphate
- Surface Total Suspended Solids
- Summer Surface Dissolved Oxygen
- Surface Water Temperature